Evaluation of complex site effects through experimental methods and numerical modelling: The case history of Arquata del Tronto, central Italy

EVALUATION OF COMPLEX SITE EFFECTS THROUGH EXPERIMENTAL METHODS AND NUMERICAL MODELLING: THE CASE HISTORY OF ARQUATA DEL TRONTO, CENTRAL ITALY

Silvia Giallini[1a, b], Alberto Pizzi[b], Alessandro Pagliaroli[b, a], Massimiliano Moscatelli[a], Gianluca Vignaroli[c, a], Pietro Sirianni[a], Marco Mancini[a], Giovanna Laurenzano[d]

a. Institute of Environmental Geology and Geoengineering - Italian National Research Council, Rome, Italy
b. Department of Engineering and Geology - University of Chieti-Pescara, Italy
c. Department of Biological, Geological and Environmental Sciences - University of Bologna, Italy
d. National Institute of Oceanography and Applied Geophysics-OGS, Trieste, Italy

Abstract: *This work deals with the experimental and numerical evaluation of the local seismic response of Arquata del Tronto area (Marche Region, central Italy), severely struck by the Mw 6.0 August 24th, 2016 earthquake. Arquata main village rises on elongated WNW-ESE-trending ridge of the central Apennines thrust-belt (central Italy), at elevations about 100 m higher than the underlying alluvial valleys where Borgo and San Francesco hamlets are built on. Despite their proximity (less than 500 meters), Arquata del Tronto, Borgo and San Francesco reported a different damage distribution after the August 2016 mainshock, suggesting that the seismic response of the area may be controlled by site effects. In order to explore this hypothesis, we evaluated the 2D numerical local seismic response along four representative geological cross-sections passing through Arquata del Tronto, San Francesco and Borgo. Additional 1D analyses were carried out at strategic points along the cross-sections in order to explore the 2D physical phenomena governing the local response. The satisfactory agreement between numerical amplification functions in linear range and experimental amplification functions obtained by the Generalized Inversion Technique (GIT) applied to a large number of aftershocks confirms the substantial reliability of the subsoil models. Numerical analyses representative of the 2016 mainshock were carried out and processed in terms of peak and key ground motion parameters. A comparison with the damage induced by the 2016 mainshock was finally undertaken substantially justifying the observed pattern. This study provides general implications about site response and seismic microzonation in sites characterized by similar complex geological and morphological settings.*

1. Introduction

The evaluation of local seismic response at sites characterized by complex geological and morphological features represents a crucial challenge. Difficulties mainly arise from both the reconstruction of a suitable and robust geological/geotechnical subsoil model and from limitations of geophysical and continuous numerical methods in such contexts (Pagliaroli et al., 2015).

Historical earthquakes in many cases showed the concentration of building damage in the villages located on the top of a relief (Paolucci, 2002), evidencing the importance of topographic amplification effects. Despite this observation, few instrumental strong motion stations are deployed on these sites and generally, when available, data show that recorded amplification is higher than numerically predicted (Geli, 1988; Pagliaroli et al., 2011). This discrepancy mainly arises from i) the difficulty to represent the complex geological and geotechnical site characteristics in the model adopted for the numerical analyses

1 *Corresponding author. E-mail address: silvia.giallini@igag.cnr.it*

(generally homogeneous media) and ii) the above-mentioned limitations of the continuous numerical models, which are not able to return the discontinuous behavior of jointed rock mass.

On August 24th, 2016, an Mw 6.0 earthquake (Azzaro et al., 2016) with epicentral area located near the village of Accumoli (Lazio Region), hit central Italy (Fig.1). The mainshock was followed by aftershocks located southeast and northwest of the epicenter, and by Mw 5.9 and Mw 6.5 seismic events occurring on 26th and 30th October, respectively, about 25 km to the NW of the previous mainshock (Fig. 1).

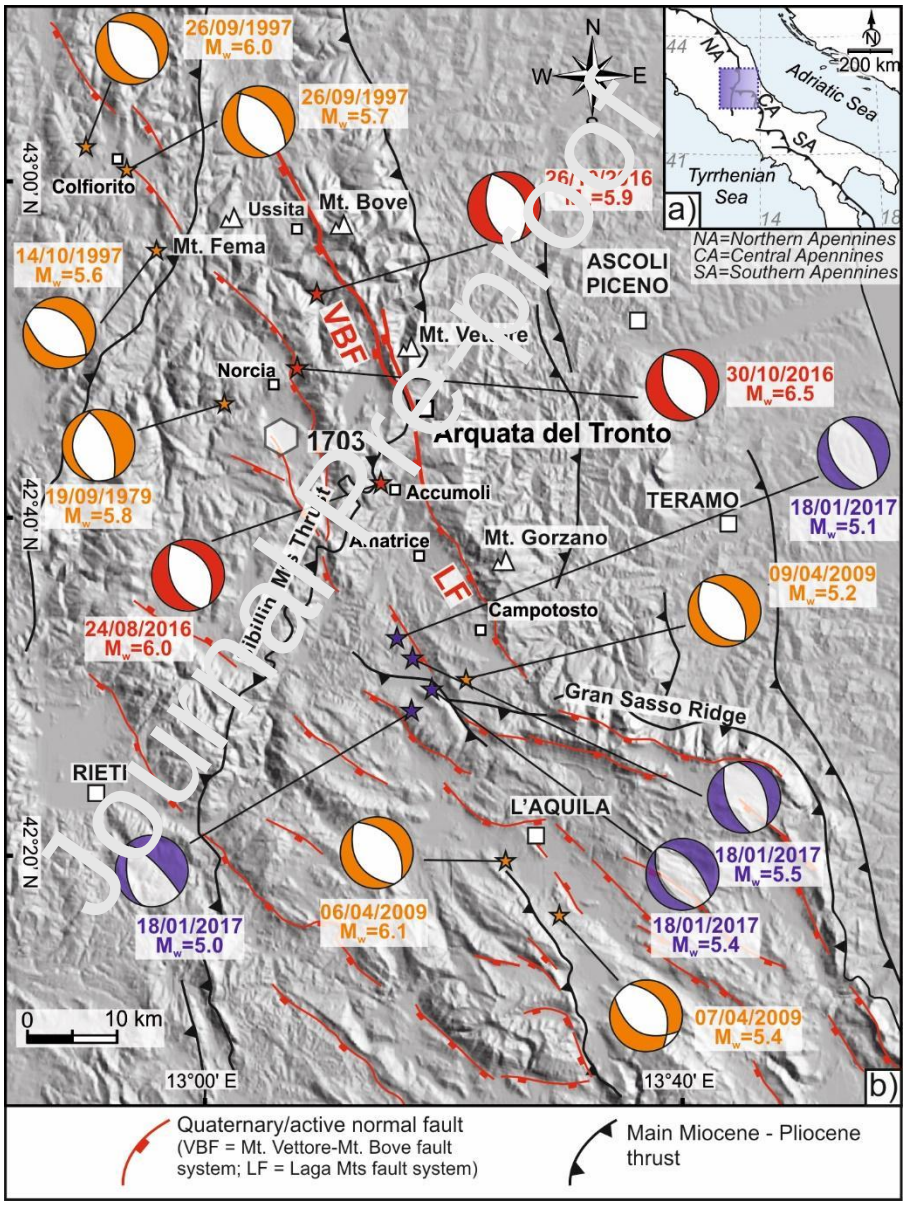

Figure 1. a) The three major arcs of the Apennine Neogene Chain. The blue rectangle indicates the study area; b) simplified structural map of the central Apennines and related seismicity with focal mechanism and moment magnitude (Mw) of historical and recent earthquakes. The hexagon indicates the epicenter of the January 14, 1703 event. In orange: focal mechanism pre-2016; in red: 2016 mainshocks; in purple: 2017 events with Mw≥5.0 (modified from Di Domenica & Pizzi, 2017).

The impact of the 2016-2017 seismic sequence and in particular of the August 24th, 2016 event was highly destructive, causing ~300 casualties and extensive and irregularly distributed damage. After the

earthquakes of 2016-2017, quantitative seismic microzonation (SM) studies were performed in order to obtain a clear background on site effects to perform a correct reconstruction of the municipalities (Pergalani et al., 2019). In particular, this paper refers the case study of some hamlets located along the Tronto River Valley where a severe and heterogeneous pattern of damage was observed, suggesting the potential role of site effects in amplifying/localizing the ground motion. Arquata del Tronto, Borgo, and San Francesco villages (all located in the Municipality of Arquata del Tronto) have been heterogeneously damaged by the August 24th, 2016 earthquake (Galli et al., 2016; Pagliaroli et al., 2019), although the distance among these three sites is less than 500 meters. Figure 2 reports a zonation of the damage distribution defined after the reconnaissance activity following the August 24th event (Lanzo et al., 2018) and some representative pictures. The damage categories proposed by Bray et al. (2000) were considered, ranging from D0 (no damage) to D5 (collapse of the structure). In particular, the level of damage increases moving from Borgo (damage D1-D2) to San Francesco (D2-D3) and Arquata del Tronto (D4-D5). Considering the quite similar vulnerability of buildings, the mutual proximity of villages, and their comparable distance from the August 24th, 2016 main shock epicenter (~9 km), the observed damage pattern could be related to changes in seismic motion caused by the particular local geological, geotechnical, and morphological conditions of the study area.

Figure 2. Damage zonation and some representative pictures taken within the villages of Arquata del Tronto and surrounding hamlets of Borgo and San Francesco after the August 24th, 2016 earthquake. Study area and pictures location are also shown.

Arquata del Tronto village is built on an elongated WNW-ESE-trending ridge in the central Apennines thrust-belt (central Italy), made of the alternation of different rocky lithofacies Late Miocene in age, partially fractured and with high angle dipping strata, characterized by strong weathering at the shallow depths, while Borgo and San Francesco rest in part on Quaternary sediments filling a valley floor. In this particular geological scenario, ground shaking may be affected by different factors: (i) stratigraphic

amplification due to shallow continental deposits resting on the bedrock; (ii) effects ascribed to the topographic features such as focusing/defocusing phenomena and resonance of the relief (Faccioli et al., 1997); (iii) coupling between topographic and stratigraphic effects or "atypical topographic effects" (Marzorati et al., 2011; Massa et al., 2014; Pagliaroli et al., 2015).

Historical documents reported that also after the Mw=6.9 Valnerina earthquake (January 9th, 1703) an increasing level of damage was observed moving from Borgo toward Arquata del Tronto ridge (VII-VIII MCS, IX MCS respectively; Rovida et al., 2016), thus confirming the possible occurrence of site effects.

This paper investigates the role of local conditions in Arquata del Tronto and in the surrounding hamlets of Borgo and San Francesco, through a multidisciplinary approach based on experimental and numerical methods, aiming at identifying the physical phenomena driving the site response and at justifying the observed irregular damage pattern.

We firstly give a short summary of the state of knowledge on complex topography site effects and a brief description of the regional geologic and seismotectonic settings. Then, the results of 1D and 2D numerical simulations obtained along four sections and at some representative points located in the three neighboring hamlets are presented. The main goal of this work is to quantitatively evaluate the irregular amplification pattern experienced during the August 24th, 2016 earthquake, to investigate the causes, and to offer a valid methodology for the evaluation of site effects in such complex configurations.

2. State of art of evaluation of topographic site effects

In the last decades, significant research efforts were devoted to the understanding of the physical phenomena causing the variability of seismic waves on isolated reliefs and across slopes. Focusing of seismic waves near the crest, interaction between incident and diffracted waves and 2D relief resonance are generally invoked to explain such wave field modifications (Geli et al., 1988; Bard, 1999; Faccioli et al., 2002). The first two phenomena generally lead to amplification at crest and an alternation of amplification and deamplification along slopes. On the contrary, 2D resonance involve the whole relief and it usually occurs for wavelengths slightly larger than the base of the hill (i.e., for dimensionless frequency <1) highlighting that topographic amplification is generally strongly frequency-dependent (Paolucci, 2002). This was confirmed by parametric studies on slope morphologies (Ashford et al. 1997; Bouckovalas & Papadimitriou, 2004). Numerical studies present in literature also show that a parasitic vertical acceleration has to be added to that of the original seismic excitation (Bouckovalas & Papadimitriou, 2004) and the amount of amplification increase for steeper topographies (Bard, 1999).

Despite the large amount of studies on topographic effects, the comparison between the recorded amplifications on reliefs and those from theoretical prediction highlighted the general failure of the numerical method to quantitatively match the observed amplification (Geli et al., 1988).

This discrepancy mainly arises from the difficulty to represent the complex geological and geotechnical site characteristics in the numerical model. As a matter of fact, many studies considered uniform media focusing essentially on the effects of the morphologic features (e.g., Gilbert & Knopoff, 1960; Hudson, 1967; Hudson & Boore, 1980) and geometric parameters such as the slope inclination and shape ratio

(e.g. Sills, 1978). Several observations in areas characterized by particular geological and morphological features highlighted the important role played by the coupled stratigraphic and topographic effects, jointly concurring in modifying the incoming motion (Spudich et al., 1996; Marzorati et al., 2011; Pagliaroli et al., 2015). Massa et al. (2014) refer to this particular condition with the term "atypical topographic effects", while the authors refer to 'topographic effects' only in the case where the ground motion amplification is mainly caused by the morphological features of the site (i.e., ridges and slopes characterized by quite homogeneous mechanical properties). In this respect, the causes of the discrepancy between observation and numerical simulation may hence primarily be associated with an oversimplification of geology beneath the relief, being more complex than the homogeneous rock usually introduced in the models (Geli, 1988; Pedersen et al., 1994; Lovati et al., 2011; Massa et al., 2014). Moreover, many numerical models consider simplified morphologies recurring to idealized triangular or trapezoidal shapes cut perpendicularly to the ridge trend, instead of more complex 2D/3D configurations.

Le Brun et al. (1999) showed that the presence on a relief of a local layer of weathered material may produce amplification at frequency not compatible with the effect of geometric features. A numerical study carried out by Graizer (2009) on the Tarzana hill (Los Angeles, California), concluded that the presence of a low velocity zone at the top of the hill underlain by relatively high velocity rock may act as a wave trap and produce resonance at the same frequency range referable to geometrical features effects. Burjánek et al. (2014) performed a systematic study on a set of sites with pronounced topography concluding that a major role in the strong systematic amplification observed is often played by the shear-wave velocity structure, rather than by the shape of the topography. Besides the presence of a low velocity zone, often linked to a near surface weathering (Steidl et al., 1996; Le Brun et al., 1999; Graizer, 2009), in many common cases the seismic response of the hill is affected by modification induced by widespread faulting/fracturing and jointed characteristics of the rock mass (Paolucci, 1999; Rovelli et al., 2002; Martino et al., 2006; Hailemikael et al., 2010; Marzorati et al., 2011, Pagliaroli et al., 2015; Vignaroli et al., 2019).

A correct quantitative evaluation of amplification at complex topographies therefore requires a detailed characterization of the subsurface structure (i.e., shear wave velocity structure and internal heterogeneities of the relief).

The limitations of the numerical models in capturing the discontinuous behavior of jointed rock mass and the difficulties in the mechanical characterization of such materials makes numerical analyses not yet effective in properly capturing the observed amplification linked to topographic complex site effects. Experimental methods may be an alternative option for site effects evaluation in complex conditions. They are subdivided into two categories: reference site and non-reference site techniques. However, reference site methods such as the Site Spectral Ratio SSR (Borcherdt, 1970) and Generalized Inversion Technique GIT (Andrews, 1986), may result sometimes not practicable, due to the difficulty to find a good reference station (i.e., site located on unweathered and flat outcropping bedrock). For this reason, non-reference techniques, such as horizontal to vertical spectral ratios (HVSR), have received an increasing attention and it is usually adopted for estimation of the fundamental resonance frequency at sedimentary sites (Lermo & Chávez-García, 1993; Bard & Riepl-Thomas, 2000). Recently, the HVSR technique, both on earthquakes and microtremors, has been applied also for the evaluation of topographic effects (Chávez-García et al., 1996, 1997; Zaslavsky & Shapira, 2000), showing encouraging results also

at complex structures and fractured rock sites and allowing to catch the preferential polarization of the amplification and the resonance frequency of the relief (Martino et al. 2006; Pagliaroli et al. 2007, 2015; Lovati et al. 2011; Marzorati et al., 2011; Pischiutta et al. 2013, 2017; Panzera et al. 2014; Hailemikael et al. 2016; Di Naccio et al. 2017).

In conclusion, we show in this paper that the join use of numerical and experimental methods can be useful in reducing the uncertainties in the quantitative evaluation of site effects at complex site (Pagliaroli et al., 2015).

3. Geological framework

The Arquata del Tronto territory is located within the Apennine Chain at the boundary between the northern and central Apennines Fold and Thrust Belt (Fig.1a) (e.g., Boccaletti et al., 1990; Doglioni, 1991).

The study area was affected by multiphased contractional and extensional deformation, which involved reactivation/inversion of previous structures (e.g., Koopman, 1983; Di Domenica et al., 2014, and references therein). Quaternary NW-SE trending normal fault systems, 15 to 35 km long, are associated to intermontane basins and present-day seismicity with historical earthquakes up to Mw 7 (e.g., Calamita & Pizzi, 1994; Galadini & Galli, 2000; Boncio et al., 2004; Pizzi & Galadini, 2009). Normal fault kinematics indicates a NE-SW directed extension that is fully consistent with the focal mechanism solutions of the events located in the northern-central Apennines, including the mainshocks of the 2016-2017 seismic sequence (Chiaraluce et al., 2017).

The study area (Fig. 1b) is located approximately 5 km south of the southeastern flank of Mt. Vettore, where the Triassic-Miocene Umbria-Marche carbonate succession is tectonically juxtaposed on to the Messinian foredeep deposits of the Laga Formation by the east-verging Sibillini Mts. thrust (Pierantoni et al., 2013). Furthermore, it is to note that Arquata del Tronto is sited in the area of stress interaction between the southern tip of the Mt. Vettore - Mt. Bove (VBF in Figure 1b) and the northern tip of the Laga active normal faults (LF in Figure 1b), responsible for the 2016-2017 seismic sequence. In particular, the relation between the extended overturned forelimb that characterizes the bedding of the Laga Formation exposed at the Arquata del Tronto and S. Francesco and those of the anticlinal structure at Borgo (Fig. 3) has been interpreted by various authors either as due to the occurrence of an ~ESE-striking, transverse structure (Koopman, 1983; Centamore et al., 1991), or related to an active N 10° oriented west-dipping normal fault (Tortorici et al., 2019).

The Laga Formation is a siliciclastic turbidite succession largely cropping out in the study area and mainly consisting of three associations of lithofacies distinguished according to their sandstone/mudstone (S/M) ratio (Centamore et al., 1991; Milli et al., 2007, Marini et al., 2016). The mudstone deposits are made of fine-grained silt- and clay-sized particles. In particular, with reference to lithotypes reported in Figure 3, LAG4c is the sandstone dominated lithofacies with S/M > 10, characterized by the prevalence of very thick beds of massive sandstone; LAG4d has a ratio $3 < S/M \leq 10$ and is generally represented by a quite regular alternation of thick beds of sandstone and medium sandstone/mudstone horizons; LAG4b shows a grain size ratio $1 < SM \leq 3$ generally given by the alternation of medium sandstone beds and massive to laminated mudstone/shale.

In the study area, the Laga Formation lithofacies are usually strongly jointed and weathered. As mentioned above, in fact, the proximity to the Sibillini Mts. thrust can be responsible for the high degree of jointing, which generally lies at a high angle in the stiffer sandstone beds and close to the bedding in the mudstone layers. This jointing is also responsible for the marked deepening of the weathered layer up to depths of 10-15 m below the ground surface.

The topography of the area strongly reflects the high-energy relief due to the peculiar position of Arquata del Tronto, placed in between the highest peak of the carbonate Umbria-Marche Apennines (i.e. Mt. Vettore, 2476 m a.s.l.) and the Tronto River valley. This morphological and structural setting, combined with the high rate of uplift that the Apennines undergo since the early Middle Pleistocene (D'Agostino et al., 2001; Pizzi, 2003), is responsible for deep fluvial downcutting which originated very steep valleys with interposed narrow and elongated reliefs. These valleys are commonly infilled by alluvial gravel, gravitational and debris-flow deposits with a variable amount of sandy-silty matrix (Mancini et al., 2019).

4. Methods

This work integrates geological, geophysical, and geomechanical approaches aimed at defining the subsoil model of the study area and to understand the reason behind the spatial variation in the damage pattern observed in the aftermath of the August 24th, 2016 central Italy event. Considering the limitations of both the numerical and experimental methods for such complex sites, as discussed in section two, our estimation of ground motion amplification was made by integrating both methods.
The adopted method includes three main steps:

- Definition of a preliminary geological model. We drew a preliminary, mainly geological, model based on: (i) a detailed geological-structural survey, carried out with the aim to constrain the nature, geometry and thickness of the lithotypes. The area we mapped is within the Arquata del Tronto Municipality and extends from the north of San Francesco hamlet to the south of Arquata del Tronto village, and encompasses the hamlets of Camartina, to the west, and Borgo, to the east, with a surface extension of about 1 km^2 (Fig. 3); (ii) in situ-geomechanical characterization, performed by using a Schmidt hammer (e.g., Aydin & Basu, 2005). It aimed to test the relationships between the uniaxial compressive strength and the lithotypes. We performed a series of in-situ measurements on sub-vertical exposures of the rock mass. We measured the hardness index by applying the push rod of the Schmidt hammer in the central part of the bedding layer. We performed multiple measurements in each site in order to perform a statistical analysis on the obtained results. Eventually, we converted the hardness index into the uniaxial compressive strength (measured in MPa) by using the conversion chart provided within the Schmidt hammer manual; (iii) pre-existing and newly acquired geological and geophysical data. In particular, data used for this study consist of down-hole (DH), Multichannel Analysis of Surface Waves (MASW), Electrical Resistivity Tomography (ERT), noise measurements (HVSR). The location of pre-existing in situ investigations is shown in Figure 3, marked with black labels. In the same figure, we also reported the location of two of the thirteen temporary seismological stations installed by the Italian National Institute of Oceanography and Applied Geophysics, hereinafter OGS, from September 30th, 2016 to February 17th, 2017 (Laurenzano et al., 2019 and Priolo et al., 2019) in

the area struck by the seismic sequence. Moreover, in this work we make use of additional HVSR from noise measurements (green labels in Figure 3) performed in the Pianella and Camartina Valley, in order to better constrain the thickness of the Quaternary covers and to evaluate the shear wave velocity profiles and the resonance frequencies. Further HVRS tests were also carried out on the Arquata del Tronto ridge with the aim to investigate preferential directions of the amplification (i.e., polarization of ground motion). In the Appendix we report all the interpreted borehole stratigraphies and DH results used to constrain the subsoil model. The original seismic microzonation studies and related data are available at www.webms.it and at https://sisma2016data.it/microzonazione/. The cumulative interpretation of these data allowed us to draw four geologic cross-section passing through the study area. In detail we drew two orthogonal sections cutting Arquata del Tronto ridge (Section 1 and Section 4, in Figure 3), and two sections transverse to the axis of the Pianella and Camartina valley, passing through San Francesco (Section 2, in Figure 3) and Borgo (Section 3 in Figure 3) villages, respectively.

- Definition of a preliminary subsoil model and its calibration in linear range. The Vs values assigned to the lithotypes were generally derived from MASW and DH tests carried out in the study area, whereas no direct investigations were available, the shear-wave velocity of lithotypes were assumed considering, when presents, DH data on equivalent lithotypes acquired in the neighboring areas (within a radius of 15 km), otherwise, considering the results of the mechanical surveys performed on the ridge. As documented by Rajabi et al. (2017), we interpreted an increasing value of the uniaxial compressive strength with higher values of shear wave velocity. Regarding the nonlinear properties in this work we adopted literature curves for cover soils, whereas rocky lithotypes, characterized by high values of stiffness, were considered as linear visco-elastic materials. Finally, by using numerical and experimental results, the preliminary subsoil model was calibrated and validated in linear range by comparing the amplification functions obtained by 1D and 2D numerical analyses, performed in this study, with the corresponding experimental functions coming from the site response analyses performed by Laurenzano et al. (2019) by using the Generalized Inversion Technique GIT (Andrews, 1986) at the temporary stations located on the Arquata del Tronto ridge (at the Fortress location) and on the valley where the hamlet of Borgo is placed (MZ80 and MZ85, respectively, in Figure 3). A complete description of the site response analysis performed in the Arquata del Tronto municipality can be found in Laurenzano et al. (2019). Here we only report that GIT analyses were performed on the ground motion recordings of the thirteen seismological stations installed in the municipalities of Arquata del Tronto and Montegallo, for approximately 5 months, when the seismic sequence was ongoing. Station MZ75, located roughly 15 km NE of Arquata del Tronto hamlet (in the Uscerno village - Montegallo municipality) and installed on geological bedrock (i.e., the arenaceous lithofacies of the Laga Formation) was identified as the reference site in virtue of its flat HVSR curve. As GIT technique was applied only to events having M<5 (maximum PGA of about 0.05g) and considering the quite high values of stiffness of the materials, the experimental amplification functions are not supposed to be affected by the material nonlinearity, thus depending only on mechanical properties in the linear range (Vs, Vp) and surficial/buried morphologic features. Accordingly, we carried out 1D and 2D linear site response analyses and we

computed results at the locations of MZ80 and MZ85 seismological stations. The 1D analyses were carried out by using the STRATA code (Kottke et al., 2013) in the frequency domain, whereas the 2D simulations were carried out by using the finite element time domain QUAD4M computer code (Hudson et al., 1994). Following this calibration step, the subsoil model was slightly updated, remaining generally consistent with direct geological, geophysical, and geotechnical information, in order to better capture the experimental response in terms of resonance frequencies and amount of amplification. In particular, slight changes have been made in the deep stratigraphic contact and for those Vs values where no direct information was available.

- Numerical modelling of August 24th, 2016 mainshock and validation of the model in non-linear range. After the calibration of the subsoil model, numerical analyses were carried out for the four sections along Arquata del Tronto, San Francesco and Borgo hamlets by using a seismic input representative of the August 24th, 2016 mainshock. In particular, a set of 7 real accelerograms was selected in order to be compatible on average, in the 0.1-1.1 s period range, with the mainshock target spectrum; the Akkar et al. (2014) ground motion prediction equation, assuming Mw 6.0 and a Joyner-Boore distance Rjb = 9 km, has been employed to reproduce the August 24th, 2016 acceleration response spectrum at outcropping flat seismic bedrock. The time-histories were extracted from the Engineering Strong-Motion Database (ESM), described in Luzi et al. (2016), by constraining the selection based on magnitude and distance reference windows, fault mechanism (consistently with the predominant mechanism in the study area) and soil-topography conditions. In detail, using a M=5.5-6.5 and distance = 0-15 km as reference window, we selected normal faults events, recorded at stations located on outcropping and flat rock conditions (i.e., subsoil class A and topography category T1 according to Italian technical code NTC18). The time-histories were scaled using factors lower than 3 to obtain the compatibility with the target spectrum. The 2D numerical analyses were carried out with QUAD4M adopting a linear equivalent strategy to model material nonlinearity. Considering the quite high stiffness of material involved, the maximum shear deformations during the mainshock were in the order of 0.02% and therefore much less than 0.1%. In this deformation range, the equivalent linear approach gives results comparable to more rigorous true nonlinear analyses. Along the cross-sections in Figures 13-16 we show the results of the 2D numerical analyses in terms of profiles of spectral amplification factors (FHa) and contours of spectral amplification ratio (SR). All parameters were computed on the horizontal component as average of the 7 simulations. In detail, the Amplification Factor (FHa) has been defined with reference to the 5% damped pseudo-acceleration elastic response spectra. It is calculated as the ratio between the integral of the pseudo-acceleration elastic response spectrum of the output motion (PSA_{out}) and the pseudo-acceleration elastic response spectrum of the input motion (PSA_{in}) in selected range of periods:

$$FHa = \frac{\int_{Ta}^{Tb} PSA_{out}(T)\,dT}{\int_{0.1}^{0.5} PSA_{in}(T)\,dT}$$

where Ta and Tb represent the limit values of the period range.

In this study, we considered three different ranges of period, following those proposed in Pergalani et al. (2019) for the study area (central Italy). The Authors, considering the building characteristics (essentially the number of floors), define the following period ranges: 0.1-0.5s; 0.4-0.8s; 0.7-1.1s. For the studied area, the most relevant range is the first one corresponding to buildings characterized by 1-4 floors.

The contours of spectral amplification ratio were computed by taking the ratio, for each value of period, between the average spectral acceleration at each surficial node and the corresponding input average spectral acceleration.

Additional 1D analyses have been carried out at selected points in order to estimate the relevance of 2D effects; FHa amplification factors from 1D simulations have been computed.

Finally, we compared our results with damage pattern observed during the August, 24th 2016 seismic event, in order to validate our model also in non-linear range

5. Results

In this section we present the results of our investigations, within paragraphs dedicated to the different phases of the activities carried out in this work.

5.1 Building the preliminary subsoil model

5.1.1 Geological survey

Geological investigations allowed us to draw a detailed geological map of the study area, about 1 km^2 in surface extension and shown in Figure 3. Observing the map, it can be see that the ridge where Arquata del Tronto village lies, is mainly elongated in WNW-ESE direction and made of the alternation of different lithotypes belonging to the Laga Formation. The lithotypes are structurally arranged in a monocline geometry (trending 45-50° and dipping to the WSW), which represents the reverse limb of an E-verging anticline. Where the mudstone-rich lithotype (LAG4b) crops out, the ridge profile is transversally affected by saddles getting it a 3D shape.

Borgo and San Francesco hamlets are located about 200-500 m north of the Arquata del Tronto village and rise on alluvial valleys (Camartina and Pianella valleys in Figure 3, respectively), where the Laga Formation is covered by up to 30-40 m thick continental Quaternary deposits, mainly consisting of debris flow and coarse fluvial deposits (Fig. 3).

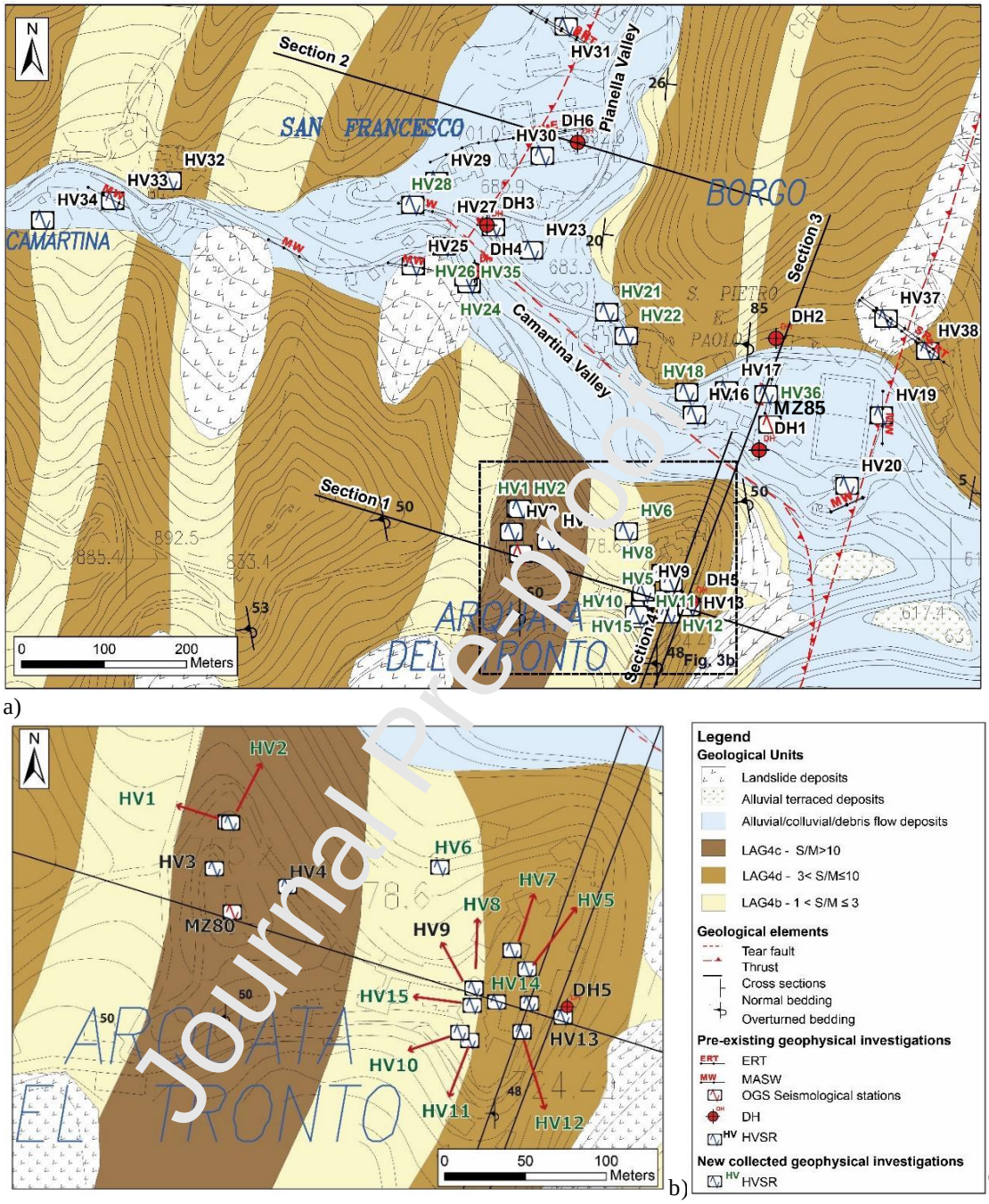

Figure 3. a) Geological map of the study area with the location of the four representative cross-sections and geophysical investigation sites used in this work.; b) an enlarged sketch of the Arquata del Tronto area (see inset in Figure 3a); c) legend of colors and symbols used in Figure 3a and b. Lithological units are described within the text.

5.1.2 Geomechanical surveys

We selected three sites across the Arquata del Tronto village named site1, site2, and site3 (Fig. 4) corresponding to the lithotypes LAG4c, LAG4b, and LAG4d, respectively. Site1 is characterized by up to 1 m-thick tabular beds of sandstones; site2 is characterized by a layering of dominant mudstone/shale with intercalation of up to 2 cm-thick layers of laminated sandstone; site3 is characterized by a rhythmic alternation of up to 10 cm-thick siltstones (site3_M3), up to 5 cm-thick claystones (site3_M4), and up to 30 cm-thick sandstones (site3_m5) (Fig. 5).

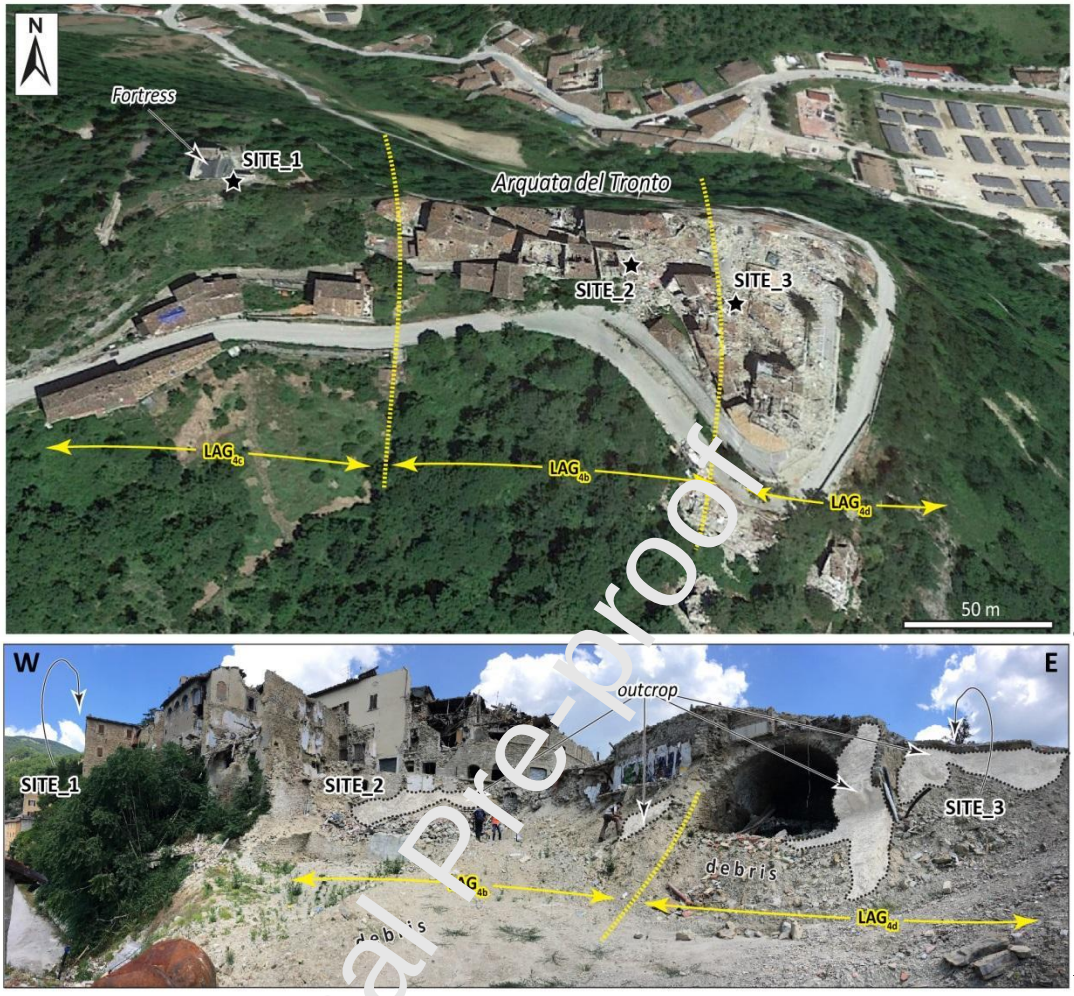

Figure 4. Google Earth© view (a) and panoramic view (b) of the Arquata del Tronto historical center, where the site locations for in-situ geomechanical measurements is shown.

Results are reported in Figure 6 in terms of hardness index. For site1, measurements show data in the range of 44-62, with Gaussian best-fit statistics of 53.8±4.7 (corresponding to uniaxial strength value of about 190 MPa). For site2, measurements show data in the range of 26-36, with Gaussian best-fit statistics of 30.5±2.6 (corresponding to uniaxial strength value of about 50 MPa). For site3_M3 (siltstones), measurements show data in the range of 31-50, with Gaussian best-fit statistics of 41.8±4.3 (corresponding to uniaxial strength value of about 110 MPa). For site3_M4 (claystones), measurements show data in the range of 31-49, with Gaussian best-fit statistics represented by two means of 34.8±1.9 and 42.7±3.8 (corresponding to uniaxial strength value of about 70 MPa and 115 MPa, respectively). For site3_M5 (sandstones), measurements show data in the range of 41-56, with a Gaussian best-fit statistics of 50.3±3.4 (corresponding to uniaxial strength value of about 165 MPa).

Summarizing, a progressive increase of the uniaxial strength value with the increasing grainsize of the bedding (from claystone to sandstone) is documented by the obtained results. This positive correlation is evident both when comparing results from different lithotypes (dominant sandstones from LAG4c in site1; claystones-siltstones-sandstones alternation from LAG4d in site3; dominant claystones from LAG4b in site2) and when comparing results from different grainsize facies within the same lithotype (claystones-siltstones-sandstones alternation from LAG4d in site3).

This correlation between lithotype and the uniaxial strength value suggests a differentiated mechanical behavior of the different lithotypes (and even of the different grainsize within the same lithotype), also in terms of stiffness, which is relevant for site response. Although additional analyses are required to confirm this trend, these preliminary results contribute to the evaluation of physical parameters that characterize the multilayer stratigraphic sequence at the Arquata del Tronto village.

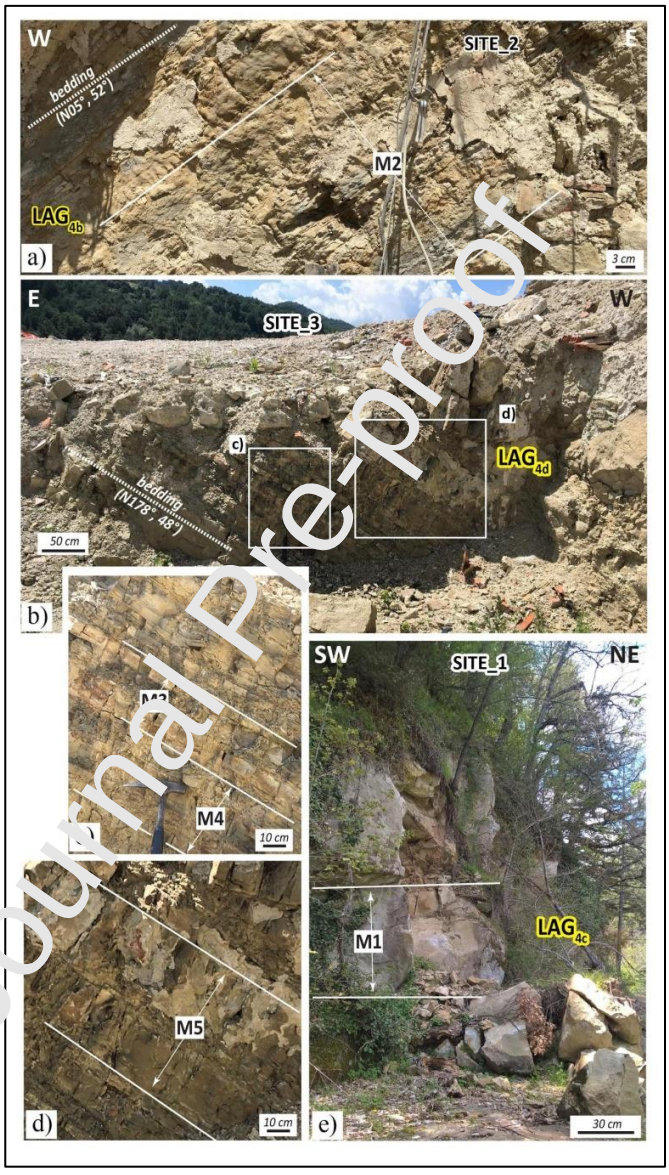

Figure 5. Outcrop details of the selected sites in LAG4b (a), LAG4d (b-d), and LAG4c (e). Labels M1-M5 represent the selected stratigraphic layers considered for in-situ geomechanical measurements.

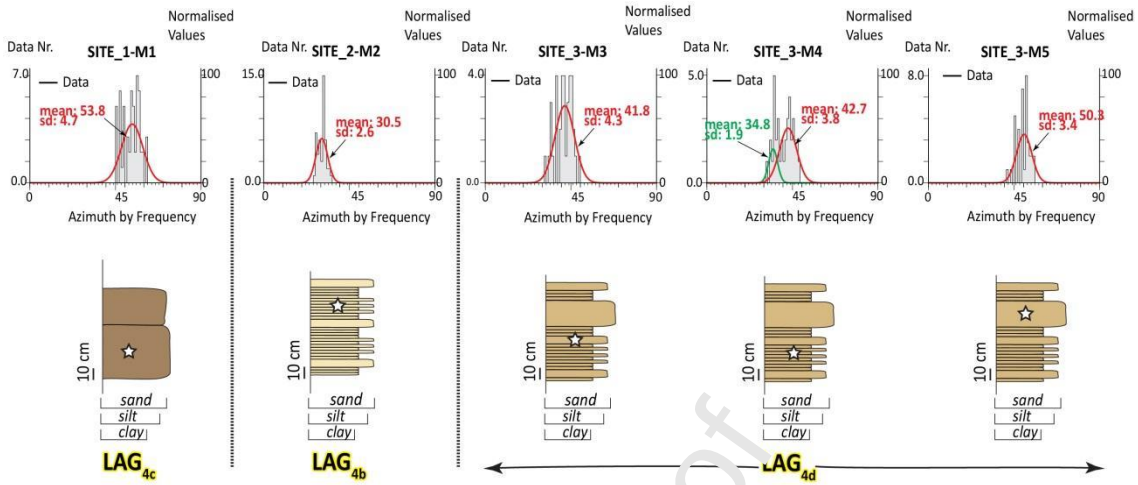

Figure 6. Relationships between lithofacies characteristics and hardness index as obtained by using the Schmidt hammer. Above, statistical analyses of the hardness index through the Gaussian best-fit statistics (the data distribution, the Gaussian curve, the mean and the standard deviation are provided). Below, schematic stratigraphic logs of the selected outcrops (the star corresponds to the bedding layer considered for measurements).

5.1.3 Collection of pre-existing data and new acquisitions

Both geognostic, geophysical, and geomechanical data available from previous studies and newer acquired specifically for this work, contributed to constrain the geometries and the thickness of the lithotypes. The results are summarized by four geologic cross-section passing through the villages of Arquata del Tronto (Section 1 and Section 4, in Figure 7a, d), San Francesco (Section 2, in Figure 7b) and Borgo (Section 3 in Figure 7c).

The HVSR curves computed from noise measurements performed along the cross-sections show at San Francesco (Fig.8a) fundamental frequencies lower than those obtained at Borgo (3.5 Hz and 6 Hz, respectively; Fig.8b). Moreover, San Francesco highlights an amplitude level of the H/V curves higher than 4 with maximum peaks of 6 and 7, whereas Borgo H/V generally drops below 4. This observation, together with information coming from geological surveys and from boreholes stratigraphy of BH1 and BH6 (shown in the Appendix and referring to DH1 and DH6 in Fig. 3), highlights that the Quaternary cover in San Francesco is thicker than in Borgo. Finally, the higher amplitude observed in the HVSR curves in San Francesco could be related to a greater impedance contrast, due to the presence of the stiff arenaceous lithotype LAG4c, as seismic bedrock in the area (Fig.7b).

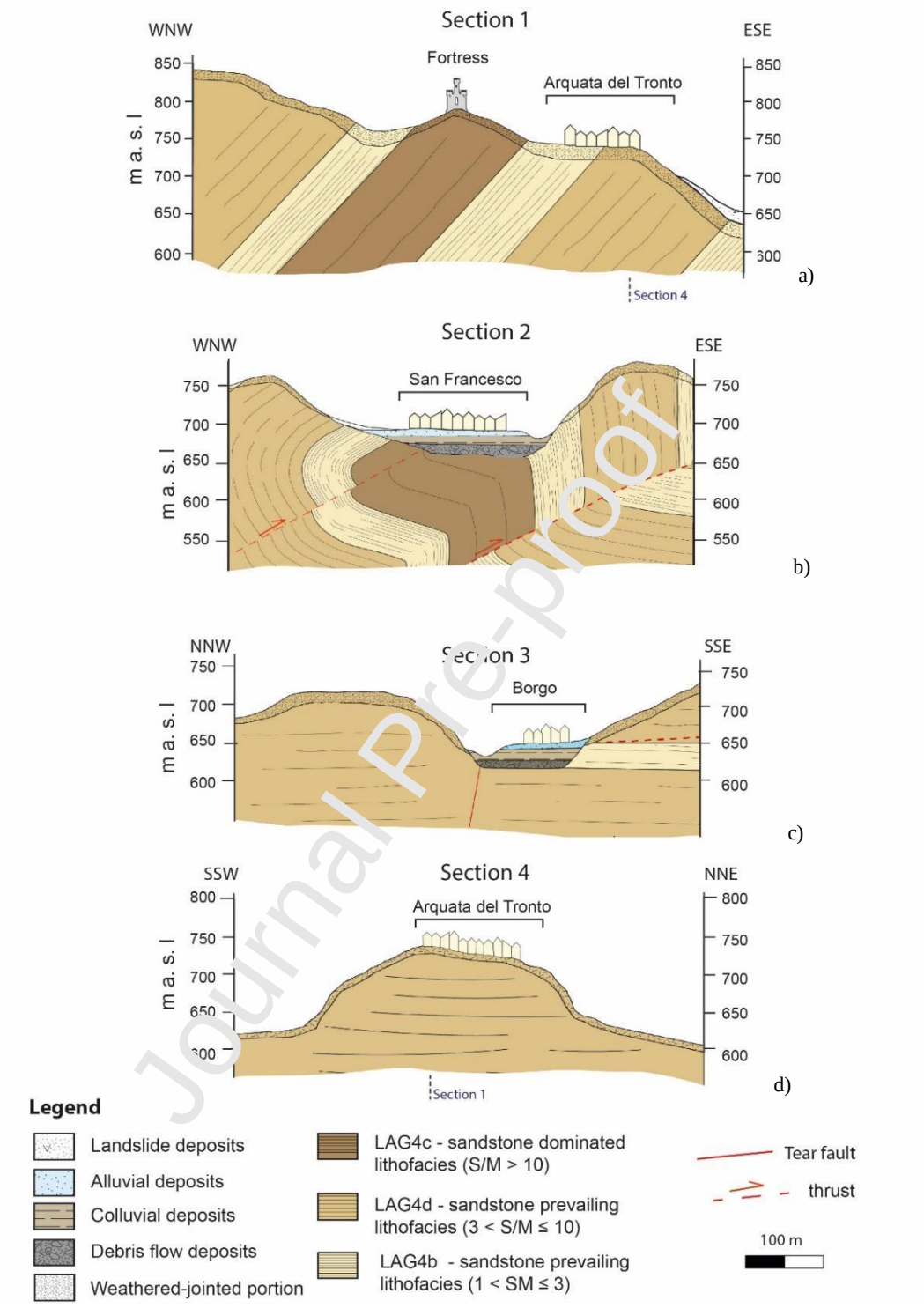

Figure 7. Cross-sections representative of the geological and structural setting of a-d) Arquata del Tronto; b) San Francesco; c) Borgo. The tracks of the-cross sections are shown in Figure 3.

Regarding noise measurements carried out at the Arquata del Tronto ridge, all HVSR curves (Fig. 8c, d, e) generally highlight the presence of multiple peaks, markers of a possible broadband amplification related to the coupling of stratigraphic and topography effects. We interpreted this phenomenon as probably linked to the upper weathered-jointed portion of different rocky lithotypes cropping out on the

ridge, as inferred by the interpretation of borehole stratigraphies and down-hole data. In particular, a borehole, and the relative down-hole, performed directly on LAG4d outcrop (BH5 and DH5 in Appendix; for the location see Fig. 3), provided information on the thickness of the upper weathered-jointed portion, about 15 m, since at a depth of about 15-16 m the DH5 test shows an increase of the shear wave velocity (Vs) from 750 m/s to 1000 m/s (Pagliaroli et al., 2019). This latter value was assigned to unweathered LAG4d lithotype.

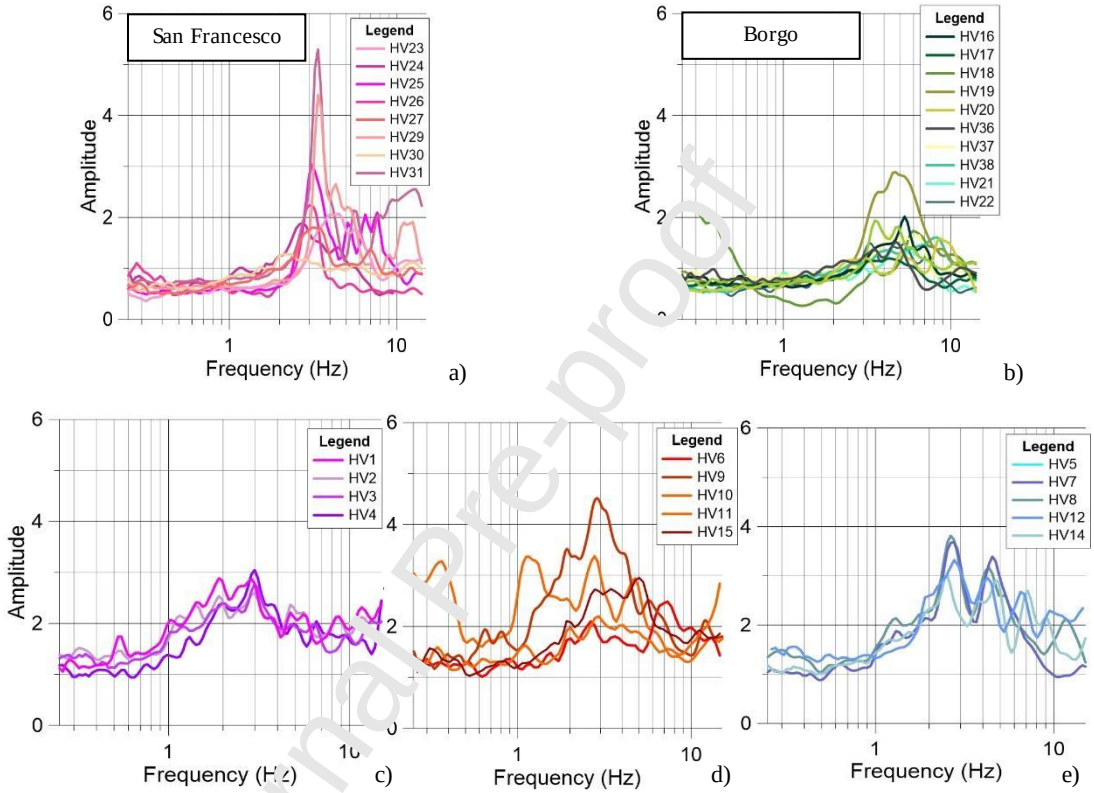

Figure 8. HVSR curves grouped according the different location where they have been recorded in: a) San Francesco; b) Borgo; c) Arquata del Tronto-LAG4c outcrop; d) Arquata del Tronto - LAG4b outcrop; e) Arquata del Tronto - LAG4d outcrop. For the location of noise measurements, see Figure 3.

Moreover, an interesting observation derives from the analysis of ground motion polarization. Figure 9 shows representative polar plots of six measures carried out on the ridge (two for each lithotype belonging to the Laga Formation). We found the presence of a different preferential roughly E-W directed polarization of the noise, in the frequency range of 2-3 Hz, in the stations situated on the WNW edge (HV1 and HV2 in Fig. 9) with respect to those located on ESE portion of the crest, directed preferentially along N-S (HV7 and HV8 in Figure 9). In some cases, the presence of two differently polarized peaks was observed for the same station (e.g., HV1 and HV8 in Fig. 9). Finally, measures taken on the center part of the ridge, show different pattern of polarization, directed both on NS and EW direction (HV 15 and HV9, respectively, in Fig.9).

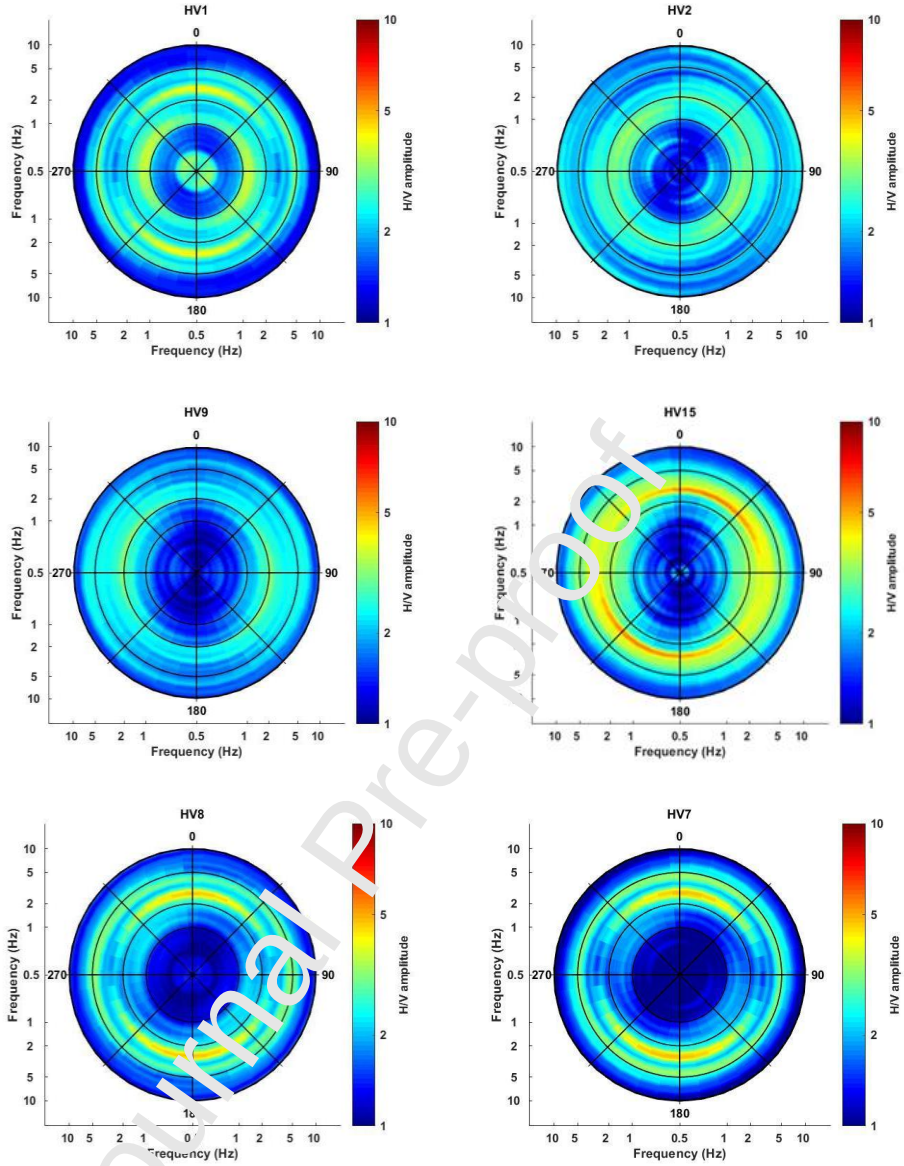

Figure 9. Polar plots, in which the amplitude is a function of both the frequency and the directional polarization (azimuths measured from the geographic North), highlighting 3D site effects affecting the behavior of the ridge. For the location of noise measurements, see Figure 3.

These findings strongly suggest that the ridge may be affected by 3D site effects.

5.2 Definition of the subsoil model and its calibration in linear range

The Vs of the less arenaceous lithotype (LAG4b) was assumed equal to 700 m/s on the basis of DH4 test (location in Figure 3; details reported in Appendix), whereas for both the weathered-jointed and intact portions the LAG4d lithotype, we derived this information from DH5 test (for the location of DH4 and DH5 see Figure 3; details are reported in Appendix). Differently, in the absence of direct investigations, the shear-wave velocity of LAG4c lithotype was assumed equal to 1200 m/s considering DH data on an equivalent lithotype acquired in the Amatrice area, 15 km south of Arquata del Tronto (CentroMS data available at www.webms.it, or at https://sisma2016data.it/microzonazione/).

Finally, having no direct measure taken on the weathered-jointed portion of the LAG4c and LAG4b lithotypes, Vs values were attributed considering the results of the mechanical surveys performed on the ridge. As we observed a progressive increasing of the UCS with the increasing grainsize of the bedding (from claystone to sandstone), taking into account Vs values directly measured on the others lithotypes of the Laga Formation, we deduced a Vs of 900 m/s and 650 m/s for the weathered-jointed LAG4c and LAG4b, respectively.

Regarding the nonlinear properties adopted in this work, literature curves for gravelly soils (Rollins et al., 1998) were employed for landslide covers and alluvial soils, given the prevalent coarse grain-size composition. Rocky lithotypes, characterized by high values of stiffness, were considered as linear visco-elastic materials with a damping ratio D in the range 0.5% -1%.

In order to verify the reliability of the subsoil model, we compared the numerical amplification functions with the corresponding experimental functions obtained by the application of the Generalized Inversion Technique (GIT) to earthquake recordings belonging to the 2016-2017 central Italy seismic sequence at the sites MZ80 (Fortress of Arquata) and MZ85 (Borgo) (Laurenzano et al., 2019). The comparisons, performed at control nodes of Section 1 and Section 3, between the results of linear 1D-2D numerical analyses and the experimental amplification functions obtained by GIT at MZ80 and MZ85 sites (black points in Fig. 11), show satisfactory agreement (Fig. 10).

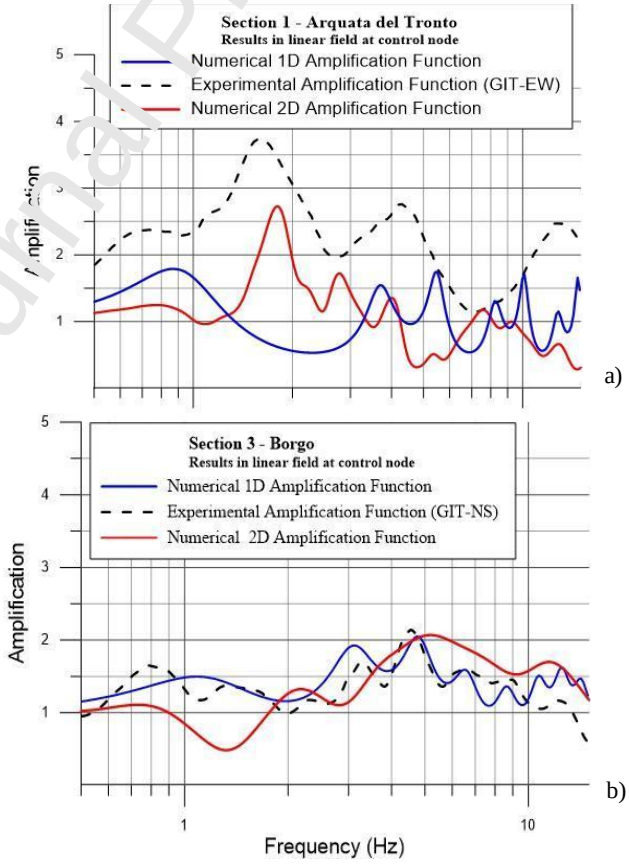

Figure 10. Calibration of the model: Comparisons between experimental results (black dotted curve) and numerical modelling (blue curve for 1D; red curve for 2D) in linear field at the control nodes located along Section 1 (Arquata del Tronto) (a) and Section 3 (Borgo) (b).

The shapes of 1D-2D and GIT amplification functions (EW component) obtained for control node in Section 1 at Arquata del Tronto ridge (Fig. 10a) are quite similar, although it is evident the higher amplification showed by the GIT curve. We have to point out that the ridge investigated is a 3D configuration and 2D analysis may slightly underestimate the response, failing in capturing the amount of the maximum amplification but adequately matching the frequency in which it occurs. A satisfactory agreement is observed between the differently computed results (Fig. 10b). In particular, 2D amplification function shows a peak with a maximum amplification of about 3 at 5.2 Hz, whereas 1D and GIT (NS component) reveal a peak of less amplitude, about 2 and 2.5, respectively, at 4.8 Hz.

We report in Table 1 the computed physical and mechanical properties of the lithotypes assumed for the four investigated sections, whereas a sketch of the 2D mesh adopted to discretize Section 1, 2, and 3 is shown in Fig. 11. It has to been pointed out that QUAD4M software models geometric damping only at the bottom of the mesh by introducing viscous dampers (absorbing boundaries). By contrast, side boundaries are perfectly reflecting; therefore, in order to reduce the influence of artificially reflected waves, side boundaries were extended about 300 m in both directions from the points of interest. As the accuracy of the solution and the computational effort are influenced by the characteristics of the mesh, the geologic model related to the examined sections was discretized through triangular finite elements, whose length, complying with Kuhlemeyer & Lysmer (1973) is smaller than one-tenth to one-eighth of the wavelength associated with the highest frequency component of the input motion.

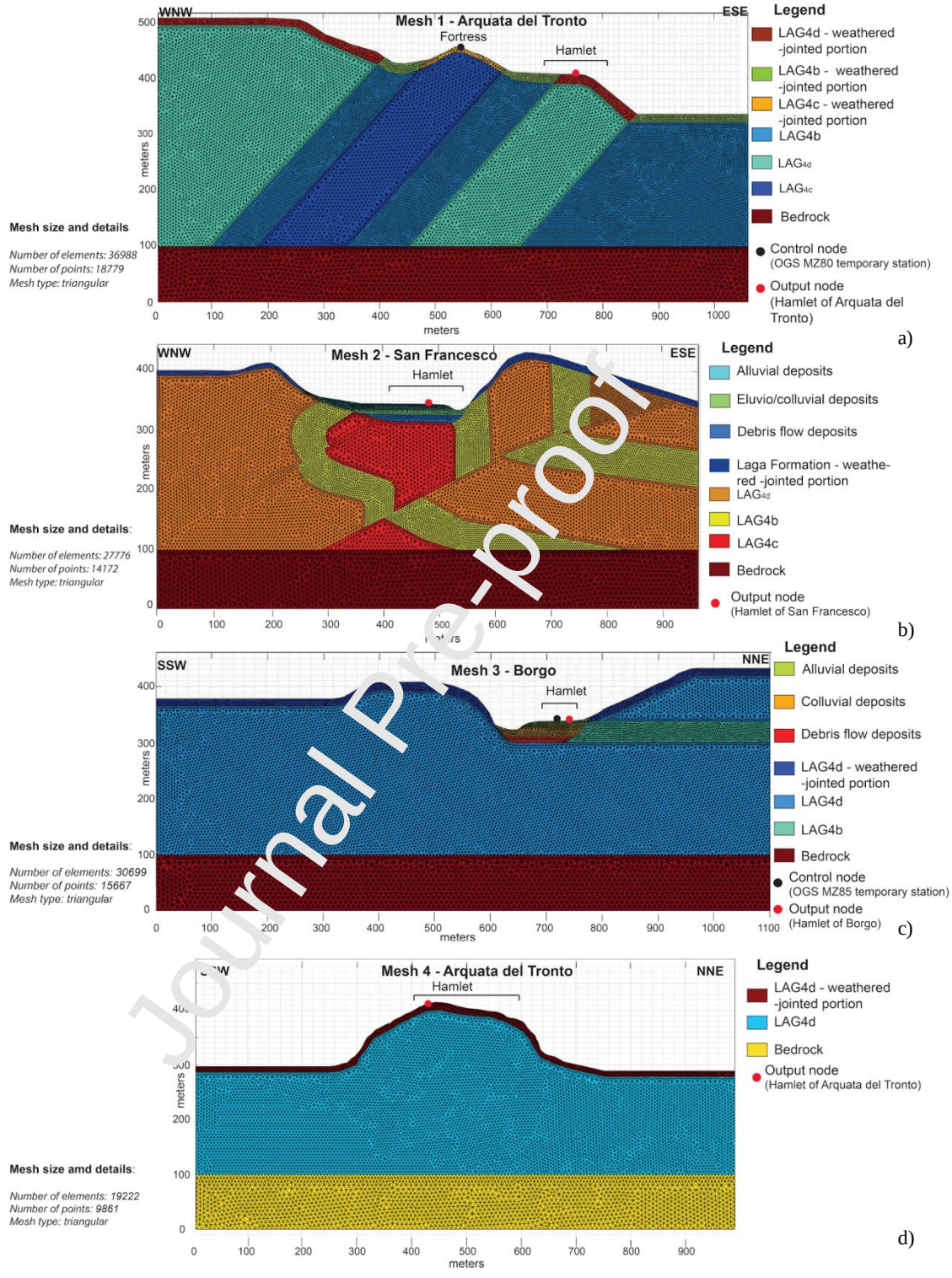

Figure 11. Finite element mesh adopted respectively for Section 1 (a), Section 2 (b) Section 3 (c) and Section 4 (d); the labels identify the lithotypes briefly described within the text, whose physical and mechanical properties are presented in Table 1. In a) and c) control nodes (black points) represent MZ80 and MZ85 OGS seismological station location, respectively named Fortress of Arquata del Tronto and Borgo; in a) b) c) and d) output node (red points) represents the hamlet center. On the left, details of the adopted meshes are also reported.

Table 1. Selected parameters for subsoil models used for site response analyses of Section 1, 2, 3, and 4

Section /site	material	γ (kN/m^3)	Vs (m/s)	ν (-)	Nonlinear curves
1 / 4 Arquata del Tronto	LAG4b	22	700	0.4	Linear D 1%
	LAG4c	23	1200	0.38	Linear D 0.5%
	LAG4d	23	1000	0.4	Linear D 1 %
	LAG4c Weathered – Jointed portion	22	900	0.4	Linear D 1%
	LAG4b Weathered – Jointed portion	21	650	0.42	Linear D 1%
	LAG4d Weathered – Jointed portion	22	750	0.4	Linear D 1%
	Bedrock	24	1500	0.36	Linear D 0.5%
2 San Francesco	LAG4b	22	700	0.4	Linear D 1%
	LAG4c	23	1200	0.38	Linear D 0.5%
	LAG4d	23	1000	0.4	Linear D 1 %
	Weathered – Jointed portion	22	750	0.4	Linear D1%
	Sandy -Silty alluvial deposit	18	400	0.42	Rollins et al. (1998)
	Silty clay eluvial – colluvial deposit	19	550	0.42	Rollins et al. (1998)
	Debris flow deposit	21	700	0.4	Rollins et al. (1998)
	Bedrock	24	1500	0.36	Linear D 0.5%
3 Borgo	LAG4b	22	700	0.4	Linear D 1%
	LAG4d	23	1000	0.4	Linear D 1 %
	LAG4d Weathered – Jointed portion	22	750	0.4	Linear D 1%
	Sandy -Silty alluvial deposit	19	400	0.42	Rollins et al. (1998)
	Colluvial deposit	21	600	0.4	Rollins et al. (1998)
	Debris flow deposit	21	820	0.4	Rollins et al. (1998)
	Bedrock	24	1500	0.36	Linear D 0.5%

5.3 Numerical modelling of August 24th mainshock and validation of the subsoil model in non-linear range

As already stated in section 4, numerical analyses were carried out by using as seismic input a set of 7 real accelerograms compatible on average with of the August 24th, 2016 mainshock. Among these 7 events, shown in Figure 12, we included two recordings of the August 24th, 2016 earthquake; one of these is a component of the recording at RQT seismic station (located 5 km northern of Arquata del Tronto hamlet) that has shown a perfect agreement with Akkar et al. (2014) target spectrum, therefore no amount of scaling has been necessary.

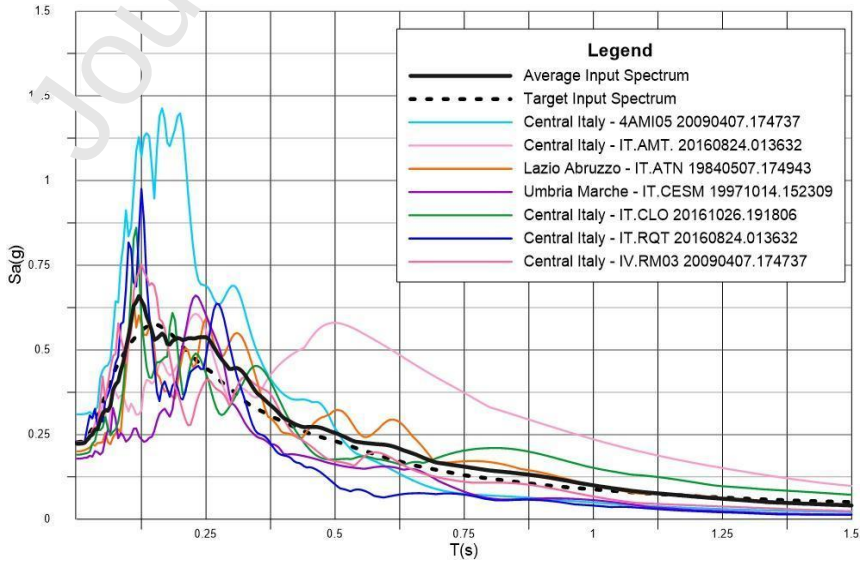

Figure 12. Response spectra input selected for the numerical analyses. The dark dotted line represents the target spectrum obtained by the application of Akkar et al. (2014) attenuation law.

At Arquata del Tronto (Fig. 13), the simulation reveals a prominent ground motion amplification (FHa ~2) in the period range of 0.4-0.7s in correspondence of the eastern edge of the ridge close to the slope

crest (Fig. 13b), whereas lower values of amplification characterize the fortress (FHa ~1.8) and the western part of the village (FHa=1.6-1.8); minor amplification values (i.e., below 1.5) characterize the others period ranges (0.1-0.5s; 0.7-1.1s). This is confirmed by looking at the contour map of the amplification spectral ratio (Fig. 13a), which highlights amplifications as high as 2 at about 0.5-0.6 s in correspondence of the Fortress and eastern portion of the village (progressive 350 m and 600 m, respectively). By considering the quite low values of 1D amplifications (Figure 13b) in these areas the ground motion is essentially driven by topographic effects. The relevance of topographic effects is confirmed by the 2D analyses carried out on the section crossing Arquata del Tronto along SSW-NNE direction (Section 4 in Fig.3). Spectral ratio and FHa present the highest values in the 0.4-0.8 s and 0.7-1.1s period range (Fig-14) well above the 1D simulations. In particular, spectral amplifications as high as 3 are reached around 0.6-0.7s therefore exceeding the amplification computed at section 1. Moreover, by comparing the results obtained at section 4 with those obtained along section 1, a relevant amplification (1.5-1.8) is also attained in the 0.1-0.5s period range; the spectral amplification clearly highlights a peak around 0.2s. The markedly different answers along the 2 sections of Arquata del Tronto ridge clearly indicate relevant 3D effects.

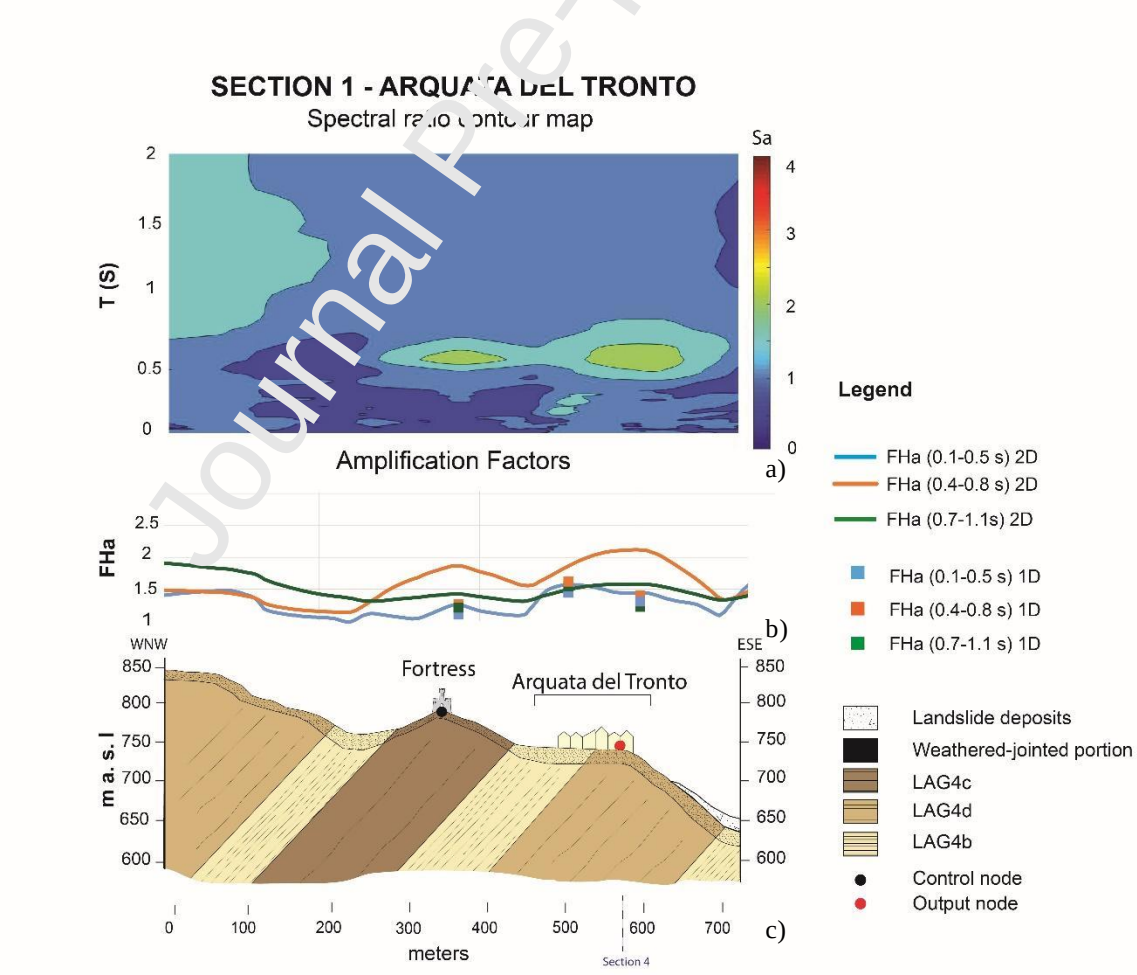

Figure 13. Results of numerical analysis in term of Spectral amplification ratio (a) and Amplification Factor (b) computed along the geological Section 1 – Arquata del Tronto (c)

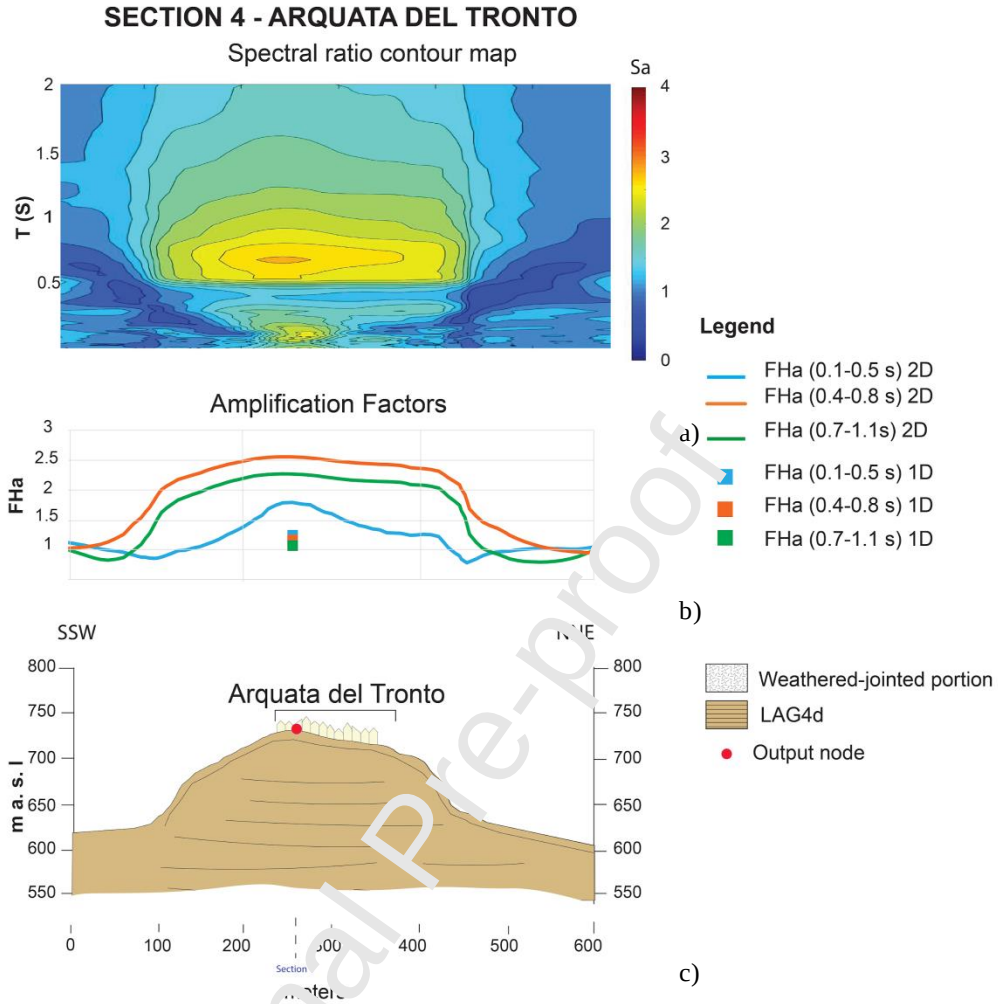

Figure 14. Results of numerical analysis in term of Spectral amplification ratio (a) and Amplification Factor (b) computed along the geological Section 4 – Arquata del Tronto (c).

At San Francesco major amplification effects take place in the 0.1–0.5 s period range (Fig.15b) where amplification of about 2.6 characterizes the eastern edge of the valley (Fig. 14b); on the other hand, values between 1.5 and 2 are achieved at the western edge. Lower values (below 1.5) are attained in the higher period ranges (0.4-0.8s; 0.7-1.1s). This observation is consistent with the trend of the values of the spectral amplification ratio showed in Fig.14a. A clear peak of amplification of about 4 characterizes the valley near its eastern edge at 350-370 m for periods around 0.2s (Fig. 15c). The combined effects of the thickness of the Holocene continental deposits resting on the stiffer lithotype of the Laga Formation (LAG4c) with surficial and buried morphology could explain the estimated amount of amplification. The significant difference between 1D and 2D amplification factors at the eastern edge highlights the relevance of 2D amplification phenomena associated with surficial and buried morphology.

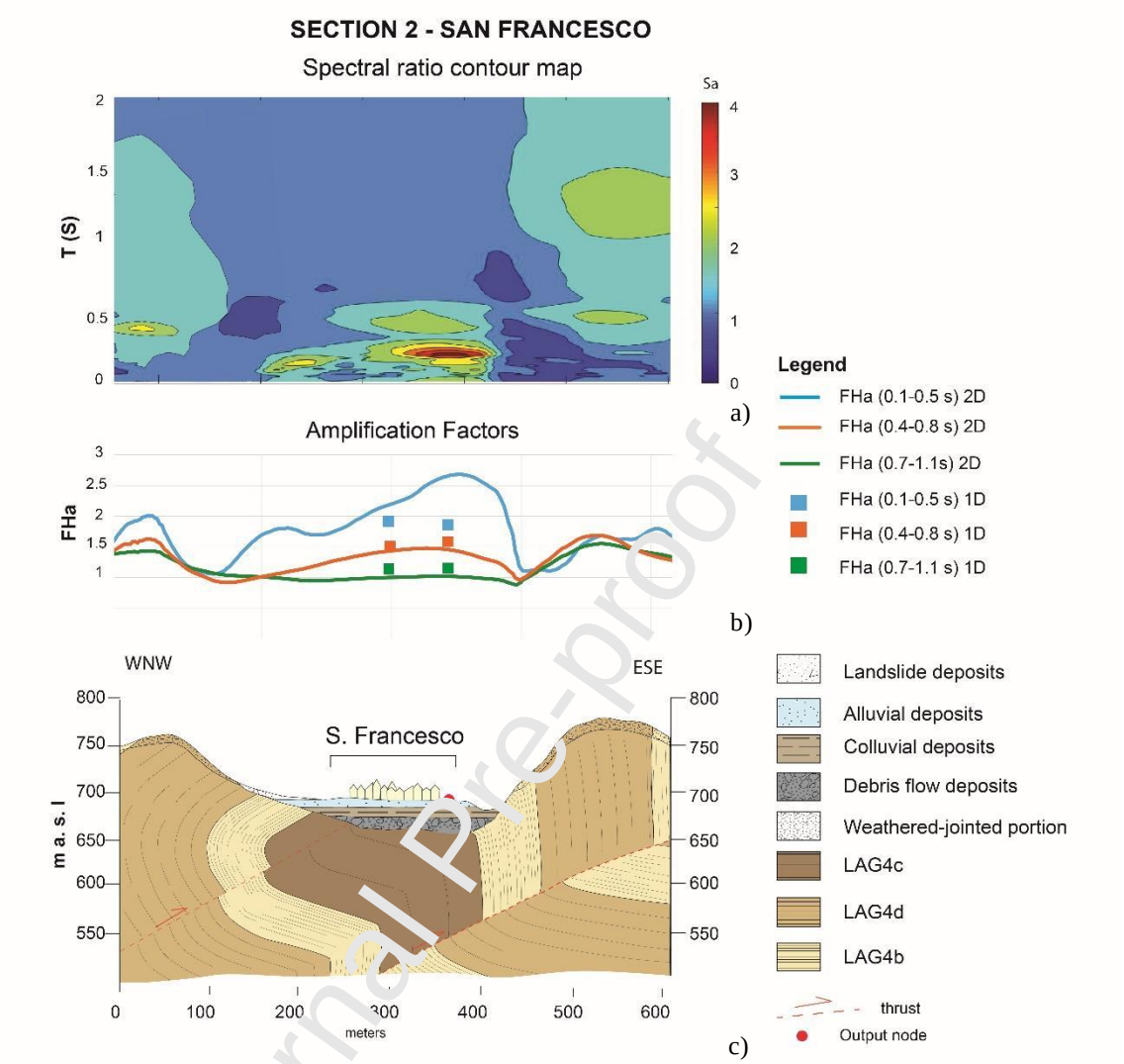

Figure 15. Results of numerical analysis in term of Spectral amplification ratio (a) and Amplification Factor (b) computed along the geological Section 2 – San Francesco (c).

Minor amplification effects (FHa ~1.6) are observed at Borgo (Fig.16b), with a peak located at the eastern side of the valley, where the hamlet is built on, in the correspondence of 0.1-0.5s period range (Fig. 16b). Here, the seismic bedrock underlying the continental deposits is the LAG4d characterized by a lower stiffness with respect to the San Francesco area. Moreover, Borgo is also characterized by a slightly lower thickness of the Holocene continental deposits than those in San Francesco. At the NNE eastern edge of the valley the LAG4b lithotype can be found having a stiffness comparable with the valley filling materials; no relevant 2D effects are therefore expected as shown by the comparison between 1D and 2D amplification factors. At higher period ranges (0.4-0.8s; 0.7-1.1s), negligible amplification values are attained at Borgo, as it is also attested by the computation of the spectral amplification ratio (Fig. 16a).

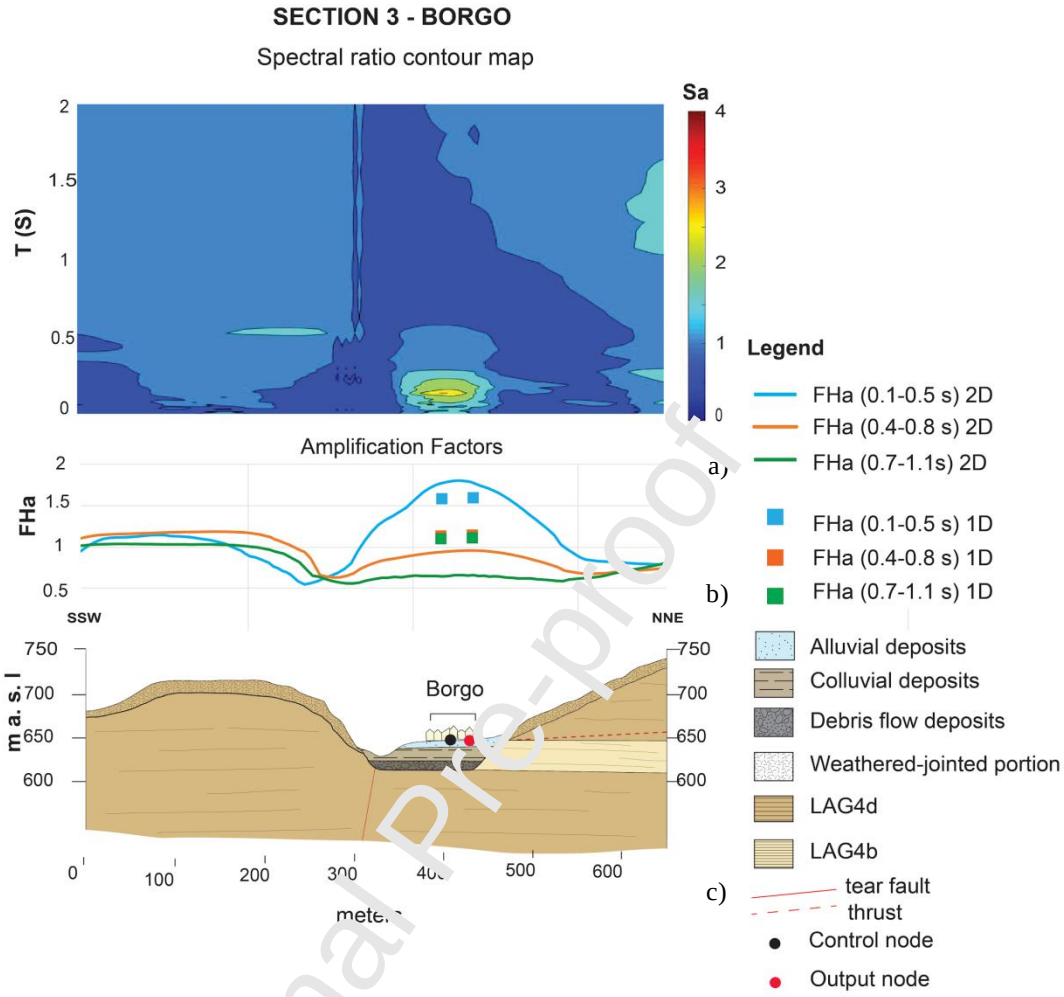

Figure 16. Results of numerical analysis in term of Spectral amplification ratio (a) and Amplification Factor (b) computed along the geological Section 3 - Borgo (c).

The results obtained at San Francesco and Borgo are substantially compatible with HVSR observations: the HVSR curves show almost flat spectral ratios for frequencies lower than 1 Hz (i.e., period > 1 s), whereas peaks appear in the frequency range of 3-8 Hz (0.1-0.3s). Moreover, higher amplitudes characterize San Francesco with respect to Borgo well matching the differences in the amplification factors computed by 2D analyses.

The same observation can be done also for Arquata del Tronto, where HVSR measurements present higher values of spectral ratio than in Borgo and San Francesco at frequency range of 1.2-2Hz corresponding at periods of 0.5-0.8s. This is consistent with the high values of amplification factor computed for the ridge along Section 1 and 4 in the period range of 0.4-0.7s. Moreover, the peaks of the HVSR acquired at Arquata del Tronto in frequency range of 2.5-6 Hz corresponding to period range of 0.15-0.4s, are reflected by numerical analyses along the section 4 while they are missing in the Section 1 simulations. Even if results from HVSR technique should be carefully considered in such complex configurations, they provided very useful information also highlighting the presence of 3D effects captured by the 2D simulations carried out on the two cross-sections 1 and 4.

In order to compare the seismic response of the three villages, nonlinear amplification functions and average acceleration response spectra for four nodes representative of the investigated villages are also reported (Fig. 17).

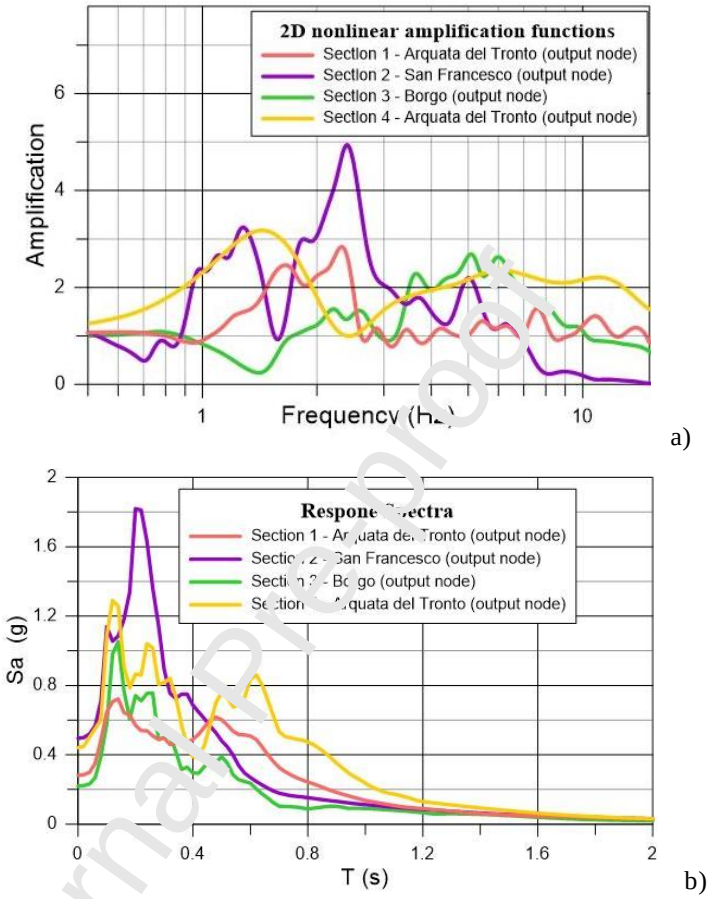

Figure 17. a, b) Simulation of the August 24th, 2016 mainshock: 2D numerical results in nodes representative (output node) of the most damaged location in Arquata del Tronto, San Francesco and Borgo. See Fig. 11 for the location of output nodes.

The investigated sites show a quite different seismic response especially in the 1-3 Hz frequency range. The highest amplification can be noticed at San Francesco (Fig.17a) where a peak of about 5 is attained at about 2.5 Hz; amplifications as high as 2-3 characterize the Arquata del Tronto ridge (calculated along Section 1 and 4; see Fig.3 for the location) while a deamplification or moderate amplification of ground motion is observed at Borgo (Fig. 17a). For frequencies higher than 3 the seismic response is more homogeneous among the three sites, being Borgo and Arquata (Section 4) characterized by higher amplifications although somewhat moderate (about 2 around 5-7 Hz).

6. Discussion

Arquata del Tronto, San Francesco and Borgo villages experienced a different degree of damage (D4-5; D2-3; D1-2, respectively in Figure 1) during the August 24th,2016 seismic event, despite their proximity (less than 500 meters) and their similar distance to the earthquake epicenter.

The villages consist mainly of unreinforced masonry structures 2–3 stories in height. Very few structures were retrofitted with through-going iron bars. Isolate relatively modern reinforced concrete structures can be found (essentially in Borgo and San Francesco). Noise measurements carried out by Pagliaroli et al. (2015) in Castelvecchio Subequo village (Abruzzi Region in central Italy) with reference to typical 2-3 stories masonry buildings like those located in the study area, showed that first vibration modes are in the range 4–6 Hz. These frequencies, estimated from ambient vibrations, characterize the building behavior in the linear range. As shown by Michel et al. (2011) a reduction up to 50 % of the vibration frequencies can take place during earthquakes because of the nonlinear behavior of masonry structures and development of cracking for severe shaking. This reduction, therefore, suggests that fundamental frequencies lies around 2-3 Hz during the most severe part of the shaking.

The response spectra in the concerned period range (0.1-0.5 s) computed at Arquata del Tronto and San Francesco (Figure 17b) could explain the high damage observed in the two villages with respect to Borgo after the August 24th mainshock (Fig. 1). Moreover, it should be noticed that the major damage occurred at Arquata del Tronto can be partially related to the vulnerability of buildings, which is slightly higher than in Borgo and San Francesco: no reinforced masonry structures were identified in the Arquata del Tronto village. In fact, iron bar-reinforced buildings, isolated concrete structures, and more recent masonry buildings were noticed only in Borgo and San Francesco. The combination of ground motion amplification and vulnerability could have played a relevant role on the significant difference in damage level observed in the three hamlets, as shown in Fig. 1. In addition, Arquata del Tronto is probably affected by 3D effects, as emphasized by the numerical results computed for two perpendicular cross-sections: the real amplification is maybe quite higher than that calculated by the numerical analyses (Fig. 17a) and comparable with or even higher than San Francesco.

Coherently with the observed damage pattern, major amplifications do occur at San Francesco and Arquata del Tronto sites. We noticed the highest amplification peak of about 5 at San Francesco whereas Arquata del Tronto ridge exhibits a peak of about 3, in the same frequencies range of 1.5-3 Hz. However, the 2D analyses could underestimate the real response at the ridge: the execution of 2D analyses on two perpendicular sections of Arquata clearly revealed 3D effects. Conversely, at Borgo the numerical analysis shows negligible amplification at 1.5-3 Hz. This frequency range is typical of masonry building similar to those located in the investigated villages, if the reduction of the vibration frequencies for the nonlinear behavior of the masonry structures is taken into account.

7. Conclusions

Local seismic response analyses were performed by using 1D and 2D numerical methods and experimental recordings (HVSR and GIT techniques) in the Arquata del Tronto area, following the heterogeneous damage pattern observed in the aftermath of the August 24th, 2016 central Italy event. In fact, despite their proximity (less than 500 meters) Arquata del Tronto, San Francesco and Borgo villages experienced a different degree of damage (D4-5; D2-3; D1-2, respectively).

The numerical results can explain the lower damage observed at Borgo with respect to Arquata del Tronto and San Francesco villages.

Regarding the physical phenomena responsible for site effects, Arquata del Tronto suffered a ground motion amplification induced by ‘‘atypical topographic effects’’ (Massa et al., 2014), which are linked to the presence of a ridge characterized by a 3D shape and the alternation of highly dipping different rocky materials and of a weathered-jointed upper layer.

On the other hand, the higher amplification observed in San Francesco rather than Borgo, lying on valleys characterized by similar morphology, may be ascribed to the different thickness and mechanical properties of the Quaternary covers, as well as the different stiffness of lithotypes representing the local seismic bedrock, resulting in a higher impedance contrast at San Francesco with respect to Borgo.

The case study here presented shows that in complex geological and morphological configurations the numerical model could be successfully calibrated by adopting a multidisciplinary approach, taking into account information coming from both geological, geomechanical, geophysical surveys and experimental methods. In particular, HVSR curves from noise measurements provided encouraging results in catching the fundamental frequency and highlighting 3D effects also in such complex configurations. Moreover, this work shows the importance of a seismological network, whose recordings could be used to obtain experimental amplification functions to apply in the calibration of reliable numerical models. This alternative may appear expensive but it is encouraged in the case of microzonation studies in regions characterized by such a complex geological, morphological, and structural setting.

Acknowledgments

Part of data used in this work reflecting the scientific research work resulted by a collaboration among: CNR -IGAG, ISPRA, POLITECNICO DI TORINO-DISEG, UNIVERSITY OF ROME "LA SAPIENZA"-DISG, UNIVERSITY OF CHIETI-PESCARA-INGEO and CNR-IAMC. We greatly thank all the members of this Working Group.

Authors are also grateful to Riccardo Bistocchi and Mirko Gattoni for sharing some borehole, downhole and HVSR data used in this work.

Funding

The present work was performed, in part, in the frame of the Art. 14 of the OCDPC394 of the 19th September 2016, funded by the Italian Department of Civil Protection (DPC) and, in part, in the frame of the project "*Microzonazione Sismica nei territori colpiti dagli eventi sismici del 2016-2017"* ordinanza n.24 of the 12th-Maggio-2017 of the Presidency of Council of Ministers. All the activities were carried out under the umbrella of the CentroMS.

Appendix: Interpreted borehole stratigraphies (BH) and downhole results (DH) used to constrain the subsoil model. Locations are reported on Figure 3. The original files can be found at https://sisma2016data.it/microzonazione/

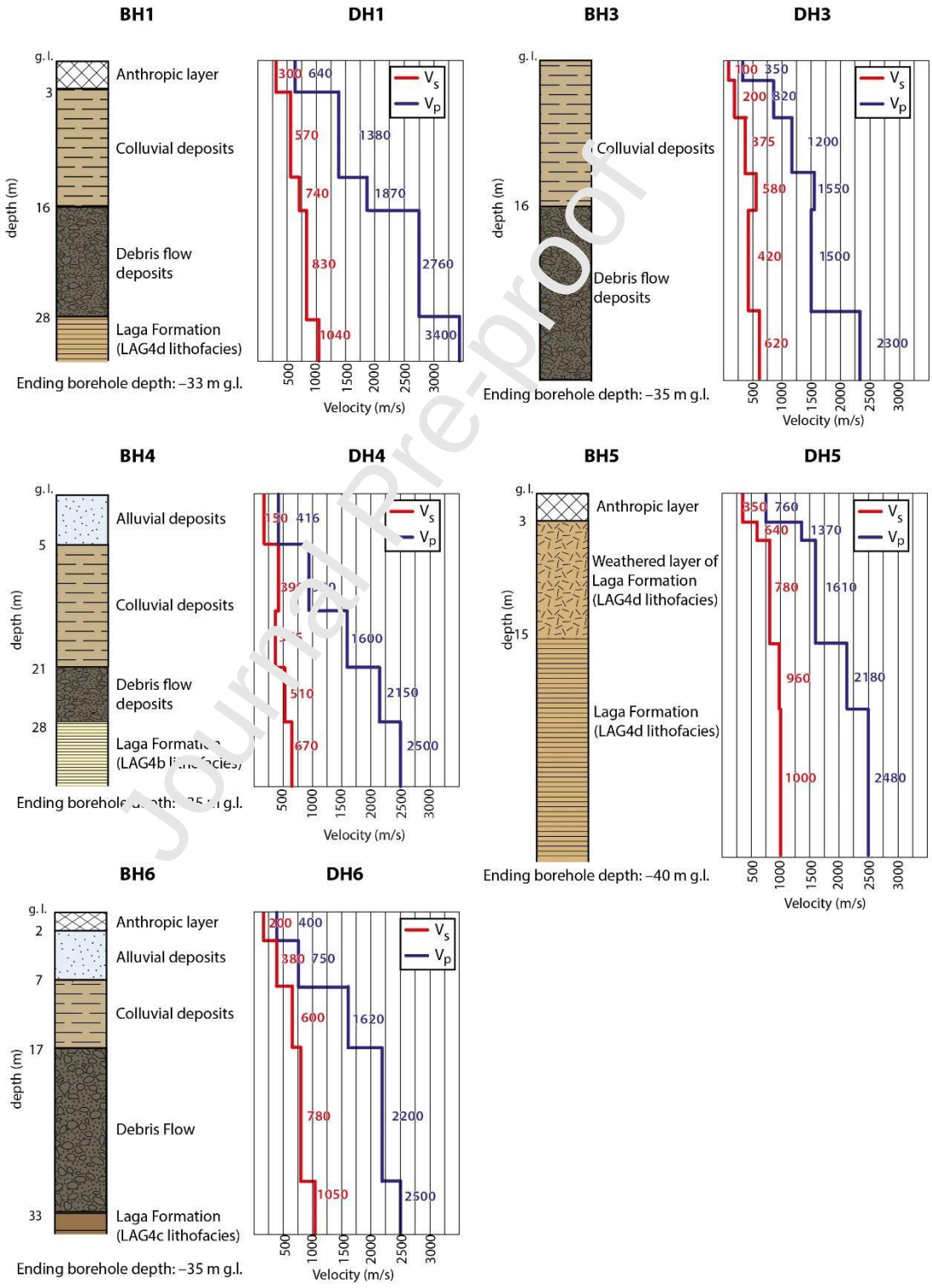

References

Akkar S, Sandikkaya MA, Bommer JJ (2014). Empirical ground-motion models for point- and extended-source crustal earthquake scenarios in Europe and the Middle East. Bull Earthquake Eng, 12(1), 359–387, doi:10.1007/s10518-013-9461-4.

Andrews DJ (1986). Objective Determination of Source Parameters and Similarity of Earthquakes of Different Size. Earthquake Source Mechanics 259-268.

Ashford S A, Sitar N, Lysmer J, Deng N (1997). Topographic Effects on the Seismic Response of Steep Slopes. Bulletin of the Seismological Society of America, 87: 701-709.

Aydin A and Basu A (2005). The Schmidt hammer in rock material characterization, Eng Geol 81:1–14.

Azzaro R, Tertulliani A, Bernardini F, Camassi R, Del Mese S, Ercolani E, Graziani L, Locati M, Maramai A, Pessina V, Rossi A, Rovida A, Albini P, Arcoraci L, Berardi M, Bignami C, Brizuela B, Castellano C, Castelli V, D'Amico S, D'Amico V, Fodarella A, Lo Schiatta I, Piscini A, Sbarra M (2016). The 24 August 2016 Amatrice earth-quake: macroseismic survey in the damage area and EMS intensity assessment. Annals of Geophysics, 59, FAST TRACK 5, 2016; DOI: 10.4401/ag-7203

Bard PY (1999) Local effects on strong ground motion: physical basis and estimation methods in view of microzoning studies. In: Proceedings of advanced study course in seismotectonic and microzonation techniques in earthquake engineering, Kefalonia, Greece.

Bard, P.Y., Riepl-Thomas, J. 2000. Wave propagation in complex geological structures and their effects on strong ground motion, Wave motion in earthquake eng., Kausel & Manolis eds, WIT Press, Southampton, Boston, 37-95.

Boccaletti M, Calamita F, Deiana G, Gelati R, Massari F, Moratti G, and Ricci Lucchi F (1990), Migrating foredeep-thrust belt systems in the Northern Apennines and southern Alps: Palaeogeography, Palaeoclimatology, Palaeoecology, v. 77, p. 41–50, doi: 10 .1016 /003-0182 (90)90097 –Q.

Boncio P, Lavecchia G, Pace B (2004). Defining a model of 3D seismogenic sources for Seismic Hazard Assessment applications: the case of central Apennines (Italy). J. Seism., 8, 407–425.

Borcherdt RD (1970). Effects of local geology on ground motion near San Francisco Bay. Bull. Seismol. Soc. Am. 60, 29–61.

Bouckovalas GD and Papadimitriou AG (2004). Numerical evaluation of slope topography effects on seismic ground motion. Proc. of 11th Int. Conf. on Soil Dynamics and Earthquake Engineering and 3th Int. Conf. on Earthquake Geotechnical Engineering, Berkeley, California, 7-9 Gennaio 2004, vol. 2: 329-335.

Bray JD and Stewart JP (2000), Chapter 8: Damage patterns and foundation performance in Adapazari. Kocaeli, Turkey Earthquake of August 17, 1999 Reconnaissance Report, Youd TL, Bardet JP and Bray JD, eds., Earthquake Spectra, Supplement A to Vol. 16, 163-189.

Burjánek J, Edwards B, F¨ah D (2014). Empirical evidence of local seismic effects at sites with pronounced topography: a systematic approach. Geophys. J. Int. (2014) 197, 608–619.

Calamita F, and Pizzi A, (1994). Recent and active extensional tectonics in the southern Umbro-Marchean Apennines (central Italy): Memorie della Società Geologica Italiana, v. 48, p. 541–548.

Centamore E, Adamoli L, Berti D, Bigi S, Bigi G, Casnedi R, Cantalamessa G, Fumanti R., Morelli C, Micarelli A, Ridolfi M, Salvucci R, Chiocchini M, Mancinelli A, Pottetti M, Chiocchini U (1991). Carta geologica dei bacini della Laga e del Cellino e dei rilievi carbonatici circostanti (Marche meridionali, Lazio nord-orientale, Abruzzo settentrionale). In: Centamore, E., Cantalamessa, G., Micarelli, A., Pottetti, M., Berti, S., Bigi, S., Morelli, C., Ridolfi, M. (Eds.), Stratigrafia ed analisi di facies dei depositi del Miocene e del Pliocene inferiore dell'avanfossa marchigiano-abruzzese e delle zone limitrofe. Studi Geologici Camerti sp, vol. 1991/2, pp. 125e135

Chávez-García FJ, Rodríguez M, Field EH, Hatzfeld D (1997). Topographic site effects. A comparison of two nonreference methods. Bull. Seism. Soc. Am., 87, 1667-1673.

Chavez-Garcia FJ, Sanchez L R, Hatzfeld D (1996). Topographic site effects and HVSR. A comparison between observations and theory. Bulletin of the Seismological Society of America, 86: 1559-1573

Chiaraluce L, Di Stefano R, Tinti E, Scognamiglio L, Michele M, Casarotti E, Cattaneo M, De Gori P, Chiarabba C, Monachesi G, Lombardi AM, Valoroso L, Latorre D, Marzorati S (2017). The 2016 Central Italy seismic sequence: a first look at the mainshocks, aftershocks and source models. Seism. Res. Lett., 88 (3), 1-15, doi:10.1785/0220160221.

D'Agostino N, Jackson JA., Dramis F, Funiciello R (2001). Interactions between mantle upwelling, drainage evolution and active normal faulting: an example from the central Apennines (Italy). Geophys. J. Int. 147, 475e497.

Di Domenica A and Pizzi A (2017). Defining a mid-Holocene earthquake through speleoseismological and independent data: implications for the outer Central Apennines (Italy) seismotectonic framework. Solid Earth, 8, 161-176, https://doi.org/10.5194/se-8-161-2017, 2017

Di Domenica A, Petricca P, Trippetta F, Carminati E, Calamita F (2014). Investigating fault reactivation during multiple tectonic inversions through mechanical and numerical modeling: An application to the central-northern Apennines of Italy. Journal of Structural Geology, 67, 167-185.

Di Naccio D, Vassallo M, Di Giulio G, Amoroso S, Cantore L, Hailemikael S, Falcucci E, Gori S, Milana G (2017). Seismic amplification in a fractured rock site. The case study of San Gregorio (L'Aquila, Italy). Phys Chem Earth 98:90–106. https://doi.org/10.1016/j.pce.2016.07.004.

Doglioni C (1991). A proposal of kinematic modeling for W-dipping subductions—Possible applications to the Tyrrhenian-Apennines system. Terra Nova, v. 3, p. 423–434, doi: 10.1111/j.1365-3121.1991.tb00172.

Faccioli E, Maggio F, Paolucci R and Quarteroni A (1997). 2D and 3D elastic wave propagation by a pseudo-spectral domain decomposition method, Journal of Seismology; volume 1, 237-251.

Faccioli E, Vanini M and Frassine L (2002). "Complex" site effects in earthquake ground motion, including topography. 12th European Conference on Earthquake Engineering, Barbican Centre, London, Uk.

Galadini F and Galli P (2000). Active tectonics in the central Apennines (Italy) – Input data for seismic hazard assessment Nat. Hazards, 22, 225–270.

Galli P, Peronace E, Tertulliani A (2016). Rapporto sugli effetti macrosismici del terremoto del 24 Agosto 2016 di Amatrice in scala MCS, Roma, rapporto congiunto DPC, CNR- IGAG.

Geli L, Bard P-Y and Jullien B (1988). The effect of topography on earthquake ground motion: a review and new results. Bulletin of the Seismological Society of America 78, 42–63.

Gilbert F and Knopoff L (1960). Seismic scattering from topographic irregularities. J. geophw Res., 65, 343 7 -3444.

Graizer V (2009). Low-velocity zone and topography as a source of site amplification effect on Tarzana hill, California, Soil Dyn. Earthq. Eng., 29, 324–332.

Hailemikael S, Lenti L, Martino S, Paciello A, Rossi D, Scarascia Mugnozza G (2016). Ground-motion amplification at the Colle di Roio ridge, central Italy: a combined effect of stratigraphy and topography. Geophys J Int 206:1–18, https://doi.org/10.1093/gji/ggw120.

Hudson JA, 1967. Scattered surface waves from a surface obstacle. Geophys. J. R. astr. Soc., 13, 441-458.

Hudson JA, Boore DM (1980). Comments on 'Scattered surface waves from a surface obstacle'. Geophys. J. R. astr. Soc., 60, 123-127.

Hudson M, Idriss IM, Beikae M (1994). QUAD4M: a computer program to evaluate the seismic response of soil structures using finite element procedures and incorporating a compliant base. Department of Civil and Environmental Engineering, University of California Davis, Davis California

Koopman A (1983). Detachment tectonics in the Central Apennines, Italy. Geologica Ultraiectina 30, 155

Kottke AR, Wang X, Rathje EM (2013). Technical Manual for Strata. Geotechnical Engineering Center Department of Civil, Architectural, and Environmental Engineering, University of Texas, 89 pp.

Kuhlemeyer RL, Lysmer J (1973) Finite element method accuracy for wave propagation problems. J Soil Mech Found Div ASCE 99(SM5):421–427

Lanzo G, Tommasi P, Ausilio E, Aversa S, Bozzoni F, Cairo R, d'Onofrio A, Durante M G, Foti S, Giallini S, Mucciacciaro M, Pagliaroli A, Sica S, Silvestri F, Vessia G, Zimmaro P (2018), Reconnaissance of Geotechnical Aspects of the 2016 Central Italy Earthquakes. Bulletin of Earthquake Engineering. https://doi.org/10.1007/s10518-018-0350-8.

Laurenzano G, Barnaba C, Romano MA, Priolo E, Bertoni M, Bragato PL, Comelli P, Dreossi I, and Garbin M (2019). The Central Italy 2016–2017 seismic sequence: site response analysis based on seismological data in the Arquata del Tronto–Montegallo municipalities. Bull Earthquake Eng. https://doi.org/10.1007/s10518-018-0355-3.

Le Brun B, Hatzfeld D, Bard PY, Bouchon M (1999). Experimental study of the ground motion on a large scale topographic hill al Kitherion (Greece). J Seism 3:1-15.

Lermo J, Chavez-Garcia FJ (1993). Site effect evaluation using spectral ratio with only one station. Bull. Seism. Soc. Am., 83, 1574-1594.

Lovati S, Bakavoli MKH, Massa M, Ferretti G, Pacor F, Paolucci R, Haghshenas E, Kamalian M (2011). Estimation of topographical effects at Nasr-i ridge (Central Italy): comparisons between experimental results and numerical modeling. Bull Earthq Eng 9:1987–2005.

Luzi L, Puglia R, Russo E and ORFEUS WG5 (2016). Engineering Strong Motion Database, version 1.0. Istituto Nazionale di Geofisica e Vulcanologia, Observatories & Research Facilities for European Seismology. doi: 10.13127/ESM.

Mancini M., Vignaroli G., Bucci F., Cardinali M., Cavinato G.P., Di Salvo C., Giallini S., Moscatelli M., Polpetta F., Putignano M.L., Santangelo M., Sirianni P. (2019) New stratigraphic constraints for the Quaternary source-to-sink history of the Amatrice Basin (central Apennines, Italy). Geological Journal, doi:10.1002/gj.3672

Marini M, Felletti F, Milli S, Patacci M (2016). The thick-bedded tail of turbidite thickness distribution as a proxy for flow confinement: Examples from Tertiary basins of central and northern Apennines (Italy). Sedimentary Geology, 341, 96-118.

Martino S, Minutolo A, Paciello A, Rovelli A, Scarascia Mugnozza G, Verrubbi V (2006). Evidence of amplification effects in fault zone related to mass jointing. Nat Hazards 39:419–449.

Marzorati S, Ladina C, Falcucci E, Gori S, Ameri G and Galadini F (2011). Site effects "on the rock": the case of Castelvecchio Subequo (L'Aquila, Central Italy), Bull Earthq Eng 9:841–868. https://doi.org/10.1007/s10518-011-9263-5.

Massa M, Barani S, Lovati S (2014), Overview of topographic effects based on experimental observations: meaning, causes and possible interpretations, Geophys J Int. doi: 10.1093/gji/ggt341.

Michel C, Zapico B, Lestuzzi P, Molina FJ, Weber F (2011), Quantification of fundamental frequency drop for unreinforced masonry buildings from dynamic tests. Earthq Eng Struct Dyn 40:1283–1296.

Milli S, Moscatelli M, Stanzione O, Falcini F (2007). Sedimentology and physical stratigraphy of the Messinian turbidite deposits of the Laga basin (central Apennines, Italy). Bollettino della Società Geologica Italiana, 126:255-281.

Pagliaroli A, Avalle A, Falcucci E, Gori S, Galadini F (2015). Numerical and experimental evaluation of site effects at ridges characterized by complex geological setting. Bulletin of Earthquake Engineering, 13:2841–2865.

Pagliaroli A, Lanzo G, D'Elia B (2011). Numerical evaluation of topographic effects at the Nicastro ridge in Southern Italy. Journal of Earthquake Engineering, 15(3), 404-432.

Pagliaroli A, Pergalani F, Ciancimino A, Chiaradonna A, Compagnoni M, De Silva F, Foti S, Giallini S, Lanzo G, Lombardi F, Luzi L, Macerola L, Nocentini M, Pizzi A, Tallini M, Teramo C (2019). Site response analyses for complex geological and morphological conditions: relevant case-histories from 3rd level seismic microzonation in Central Italy. Bull Earthq Eng. Special Issue on "Seismic Microzonation of Central Italy". https://doi.org/10.1007/s10518-019-00610-7.

Pagliaroli A, Pitilakis K, Chavez-Garcia F, Raptakis D, Apostolidis P, Ktenidou OJ., Manakou M., Lanzo G (2007). Experimental study of topographic effects using explosions and microtremors recordings. 4th international conference on earthquake geotechnical engineering june 25-28, 2007 paper no. 1573.

Panzera F, Pischiutta M, Lombardo G, Monaco C, Rovelli A (2014). Wavefield polarization in fault zones of the western flank of Mt. Etna: observations and fracture orientation modelling. Pure Appl Geophys 171:3083–3097. https://doi.org/10.1007/s00024-014-0831-x

Paolucci R (2002), Amplification of earthquake ground motion by steep topographic irregularities. Accepted for publication, in Earthquake Engineering and Structural Dynamics

Paolucci R, Faccioli E, Maggio F (1999). 3D Response analysis of an instrumented hill at Matsuzaki, Japan, by a spectral method. Journal of Seismology 3: 191–209, 1999

Pedersen H, Le Brun B, Hatzfeld D, Campillo M, Bard PY (1994). Ground-motion amplitude across ridges. Bull. Seism. Soc. Am., 84, 1786-1800.

Pergalani F, Pagliaroli A, Bourdeau C,.Compagnoni M, Lenti L, Lualdi M, Madiai C, Martino S, Razzano R, Varone C, Verrubbi V (2019). Seismic microzoningmap: approaches, results and applications after the 2016-2017 Central Italy seismic sequence. Bulletin of Earthquake Engineering https://doi.org/10.1007/s10518-019-00540-1

Pierantoni P, Deiana G, Galdenzi S (2013). Stratigraphic and structural features of the Sibillini mountains (Umbria-Marche Apennines, Italy). Italian Journal of Geosciences, 132(3), 497–520.

Pischiutta M, Fondriest M, Demurtas M, Magnoni F, Di Toro G, Rovelli A (2017). Structural control on the directional amplification of seismic noise (Campo Imperatore, Central Italy). Earth Planet Sci Lett 471:10–18. https://doi.org/10.1016/j.epsl.2017.04.017.

Pischiutta M, Rovelli A, Salvini F, Di Giulio G, Ben-Zion Y (2013). Directional resonance variations across the Pernicana fault, Mt.Etna, in relation to brittle deformation fields. Geophys J Int 193:986–996. https://doi.org/10.1093/gji/ggt031.

Pizzi A (2003). Plio-Quaternary uplift rates in the outer zone of the central Apennines fold-and-thrust belt, Italy. Quat. Int. 101e102, 229e237.

Pizzi A, Galadini F, (2009). Pre-existing cross-structures and active fault segmentation in the northern-central Apennines (Italy). Tectonophysics 476, 304e319.

Priolo E, Pacor F, Spallarossa D, Milana G, Laurenzano G, Romano MA, Felicetta C, Hailemikael S, Cara F, Di Giulio G, Ferretti G, Barnaba C, Lanzano G, Luzi L, D'Amico M, Puglia R, Scafidi D, Barani S, De Ferrari R, Cultrera G (2019). Seismological analyses of the seismic microzonation of 138 municipalities damaged by the 2016–2017 seismic sequence in Central Italy. Bull Earthq Eng https://doi.org/10.1007/s10518-019-00652-x.

Rajabi AM, Hosseini A, Heidari A (2017). The New Empirical Formula to Estimate the Uniaxial Compressive Strength of Limestone; North of Saveh a Case Study. Journal of Engineering Geology, Vol. 11, No. 3, Autumn 2017.

Rollins KM, Evans MD, Diehl NB & Daily III, W. D. (1998). Shear modulus and damping relation-ships for gravels. Journal of Geotechnical and Geoenvironmental Engineering, 124(5): 396-405.

Rovelli A, Caserta A, Marra F, Ruggiero V (2002). Can seismic waves be trapped inside an inactive fault zone? The case study of Nocera Umbra, Central Italy. Bull Seismol Soc Am 92(6):2217–2232.

Rovida A, Locati M, Camassi R, Lolli B, Gasperini P (eds) (2016). CPTI15, the 2015 version of the Parametric Catalogue of Italian Earthquakes. Istituto Nazionale di Geofisica e Vulcanologia. doi:http://doi.org/10.6092/INGV.IT-CPTI15.

Sills LB (1978). Scattering of horizontally polarized shear waves by surface irregularities. Geophys. J. R. astr. SOC., 54, 319-348.

Spudich M, Hellweg M, Lee W H K (1996). Directional Topographic Site Response at Tarzana Observed in Aftershocks of the 1994 Northridge, California, Earthquake: Implications for Mainshock Motions. Bulletin of the Seismological Society of America, Vol. 86, No. 1B, pp. S193-$208, February 1996.

Steidl JH, Tumarkin AG, Archuleta RJ (1996). What is a reference site? Bulletin of the Seismological Society of America, 86: 1733-1748.

Tortorici G, Romagnoli G, Grassi S, Imposa S, Lombardo G, Panzera F, Catalano S (2019). Quaternary negative tectonic inversion along the Sibillini Mts. thrust zone: the Arquata del Tronto case history (Central Italy). Environmental Earth Sciences https://doi.org/10.1007/s12665-018-8021-2

Vignaroli G, Giallini S, Polpetta F, Sirianni P, Gaudiosi I, Simionato M, Razzano R, Pagliaroli A, Moscatelli M, Mancini M, Cavinato GP, Avalle A (2019). Domains of seismic noise response in faulted limestone (central Apennines, Italy): insights into fault-related site effects and seismic hazard. Bulletin of Engineering Geology and the Environment 78: 2749. https://doi.org/10.1007/s10064-018-1276-8

Zaslavsky Y, Shapira A (2000). Experimental study of topographic amplification using the Israel Seismic Network. Journal of Earthquake Engineering, 4, 43-65, 2000.

AUTHORS STATEMENT FOR PUBLICATION

Manuscript title: EVALUATION OF COMPLEX SITE EFFECTS THROUGH EXPERIMENTAL METHODS AND NUMERICAL MODELLING: THE CASE HISTORY OF ARQUATA DEL TRONTO, CENTRAL ITALY

Corresponding author's full name: Silvia Giallini

Silvia Giallini: Conceptualization, Methodology, Validation, Formal analysis, Investigation, Writing – Original Draft, Writing - Review & Editing, Data Curation, Visualization; **Alberto Pizzi:** Conceptualization, Writing - Review & Editing, Supervision; **Alessandro Pagliaroli**: Conceptualization, Writing – Original Draft, Visualization, Supervision; **Massimiliano Moscatelli:** Conceptualization, Writing - Review & Editing, Visualization; **Gianluca Vignaroli:** Investigation, Formal analysis, Writing - Review & Editing; **Pietro Sirianni**: Investigation, Data Curation, Writing - Review & Editing; **Marco Mancini**: Investigation, Writing - Review & Editing; **Giovanna Lorenzano**: Investigation, Review & Editing.

To the best of my knowledge everybody who participated substantially in the study is not omitted from the article
To the best of my knowledge, all persons listed as authors qualify for authorship.
All persons who have made substantial contributions to the work but do not meet the criteria for authorship are listed in Acknowledgments section (technical help, writing assistance, general support, financial and material support)
Date
03/04/2020 Silvia Giallini, on behalf of all Authors

Declaration of interests

☒ The authors declare that they have no known competing financial interests or personal relationships that could have appeared to influence the work reported in this paper.

☐The authors declare the following financial interests/personal relationships which may be considered as potential competing interests:

HIGHLIGHTS

- Numerical modelling (1D and 2D) and experimental methods applied for the evaluation of seismic local response due to complex site effects
- Experimental amplification functions applied in the calibration of reliable numerical models
- A comparison between the response of numerical and experimental results with the damage induced by the 2016 mainshock, justifying the observed pattern
- Encouraging results of curves from noise measurements in catching the fundamental frequency and highlighting 3D effects also in such complex configurations